JBC Papers in Press. Published on September 16, 2015 as Manuscript M115.677195
The latest version is at http://www.jbc.org/cgi/doi/10.1074/jbc.M115.677195



# Identification of middle chain fatty acyl-CoA ligase responsible for the biosynthesis of 2-alkylmalonyl-CoAs for polyketide extender unit

**Takeshi Miyazawa[a,b], Shunji Takahashi[a,1], Akihiro Kawata[b], Suresh Panthee[a], Teruo Hayashi[a], Takeshi Shimizu[a], Toshihiko Nogawa[a], and Hiroyuki Osada[a,b,1]**
[a]RIKEN Center for Sustainable Resource Science, Chemical Biology Research Group, Saitama 351-0198, Japan
[b]Graduate School of Science and Engineering, Saitama University, Saitama 338-8570, Japan

**Running title:** Middle chain fatty acyl-CoA ligase involved in reveromycin A biosynthesis

[1]To whom correspondence should be addressed. E-mail: shunjitaka@riken.jp, hisyo@riken.jp

**Key words:** Biosynthesis, enzyme catalysis, secondary metabolite, natural product, polyketide
Other key words: Acyl-CoA ligase, alkylmalonyl-CoA, reveromycin, *Streptomyces*

**Background:**
Fatty acyl-CoA ligases involved in polyketide biosynthesis remain uncharacterized.
**Result:**
RevS classified in fatty acyl-AMP ligase clade was middle chain fatty acyl-CoA ligase
**Conclusion:**
RevS was responsible for 2-alkylmalonyl-CoA biosynthesis through enzyme coupling with RevT reductase/carboxylase.
**Significance:**
2-Alkylmalonyl-CoA biosynthesis was strongly supported by the function of RevR and RevS, which utilized fatty acids derived from *de novo* biosynthesis and degradation products, respectively.

## Abstract
Understanding the biosynthetic mechanism of the atypical polyketide extender unit is important to develop bioactive natural products. Reveromycin (RM)-derivatives produced by *Streptomyces* sp. SN-593 possess several aliphatic extender units. Here, we studied the molecular basis of 2-alkylmalonyl-CoA formation by analyzing the *revR* and *revS* genes, which form a transcriptional unit with the *revT* gene, a crotonyl-CoA reductase/carboxylase homolog. We mainly focused on uncharacterized adenylate-forming enzyme (RevS). *revS* gene disruption resulted in the reduction of all RM-derivatives, while reintroduction of the gene restored the yield of RMs. Although RevS was classified in the fatty acyl-AMP ligase (FAAL) clade based on phylogenetic analysis, biochemical characterization revealed that the enzyme catalyzed middle chain fatty acyl-CoA ligase (FACL) but not FAAL activity, suggesting the molecular evolution for acyl-CoA biosynthesis. Moreover, we examined the *in vitro* conversion of fatty acid into 2-alkylmalonyl-CoA using purified RevS and RevT. The coupling reaction showed efficient conversion of hexenoic acid into butylmalonyl-CoA. RevS efficiently catalyzed C8-C10 middle chain FACL activity, therefore, we speculated that the acyl-CoA precursor was truncated via β-oxidation and converted into (*E*)-2-enoyl-CoA, a RevT substrate. To determine whether the β-oxidation process is involved between RevS and RevT reaction, we performed the feeding experiment using [1,2,3,4-$^{13}$C]octanoic acid. $^{13}$C NMR analysis clearly demonstrated incorporation of the [3,4-$^{13}$C]octanoic acid moiety into the structure of RM-A. Our results provide insight into the role of uncharacterized RevS homologs that may catalyze middle chain FACL to produce a unique polyketide extender unit.

## Introduction
Microorganisms harbor structurally diverse natural products, including polyketides, peptides, and terpenoids (1). Their secondary metabolites with strong biological activity have been utilized as

antibiotics, antitumor drugs, immunosuppressants, hypercholesterolemia drugs, and insecticides (2). Unique chemical structures are linked to a variety of biological activities, therefore, understanding the biosynthetic machinery is important for future combinatorial biosynthesis (3-5).

Fatty acyl chains found in microbial natural products are responsible for biological activity and physiological function in microorganism. For instance, daptomycin binds to the cell membranes of Gram-positive bacteria through its lipid moiety, followed by calcium-dependent insertion and oligomerization (6). Dimerization of alkyl resorcinol results in the generation of potent proteasome inhibitors, cylindrocyclophanes (7). The fatty acyl chain of mycolic acid plays an important role in membrane construction in *Mycobacterium tuberculosis* (8).

Fatty acyl-AMP ligase (FAAL), a member of the adenylate-forming enzyme superfamily (9), catalyzes ATP-dependent formation of acyl-AMP and loading onto the phosphopantetheine arm of acyl carrier protein (ACP). FAALs are associated with the polyketide synthase (PKS) and nonribosomal peptide synthetase (NRPS) gene clusters, and the resulting fatty acyl-ACP is incorporated into the starter unit of the PKS and NRPS assembly line (7,10-21). In contrast to FAAL, fatty acyl-CoA ligase (FACL) catalyzes ATP-dependent conversion of fatty acid into fatty acyl-CoA through an acyl-AMP intermediate. The activated fatty acyl-CoA is utilized for phospholipid synthesis, energy generation, transcriptional regulation, and protein acylation (22,23). However, involvement of FACL in the supply of available fatty acyl-CoA for PKS extender unit remains unclear. Atypical extender units are incorporated into polyketide structures through a variety of biosynthetic pathways (24-32). Among the related enzymes, crotonyl-CoA carboxylase/reductase (CCR) homologs which catalyze reductive carboxylation of α,β-unsaturated acyl-CoA/ACP have been extensively characterized as an essential step (Fig. 1A).

Reveromycin A (RM-A) is a polyketide compound produced by *Streptomyces* sp. SN-593 (33). It inhibited bone resorption by inducing apoptosis in osteoclasts (34). The activity was also linked to the inhibition of osteolytic bone metastasis induced by lung and prostate cancer cells (34-37). *Streptomyces* sp. SN-593 produces various RM-derivatives, including RM-A (**1**), -C (**2**), -D (**3**), and -E (**4**) (Fig. 1A), whose structural diversity is derived from incorporation of atypical extender units such as butylmalonyl-CoA, isobutylmalonyl-CoA, pentylmalonyl-CoA, and hexylmalonyl-CoA, respectively. In our previous study, we identified **1** biosynthetic gene cluster possessing RevT, a CCR homolog (38). Although the presence of the *revT* gene strongly suggested the production of 2-alkylmalonyl-CoA for RM biosynthesis, we identified the *revR* and *revS* genes, which are associated in the same transcriptional unit (Fig. 1B) (38). Moreover, each gene homolog was also found in several biosynthetic gene clusters that produce polyketide compounds, including the atypical extender unit (Fig. 1) (27-32). Thus, we predicted an important role for the production of 2-alkylmalonyl-CoA by RevR and RevS, whose genes were annotated to be β-ketoacyl-[acyl carrier protein (ACP)] synthase III (KASIII) and adenylate-forming enzyme family, respectively.

In this study, we examined the molecular basis of 2-alkylmalonyl-CoA formation for RM biosynthesis through gene disruption, kinetic analysis, and precursor feeding experiments. Our results indicated that RevR is important for selective production of **1** via *de novo* fatty acid synthesis, and that RevS may represent a novel class of FACLs associated with the fatty acid degradation process, providing insight into the dynamics of fatty acid metabolism for polyketide biosynthesis. Moreover, the identification of RevS function sheds light on unexplained RevS homologs found in other polyketide biosynthetic gene clusters.

## Experimental procedures

*Chemicals and Enzymes*—Ampicillin, kanamycin, chloramphenicol, and CoA were purchased from Nacalai Tesque, Inc. (Kyoto, Japan). Streptomycin, spectinomycin, thiostrepton, ATP, NADH, NADPH, Tris (2-carboxyethyl) phosphine (TCEP), myokinase, pyruvate kinase,

and lactate dehydrogenase were purchased from Sigma-Aldrich (St. Louis, MO, USA). All fatty acids used in this study were purchased from Tokyo Chemical Industry Co., Ltd. (Tokyo, Japan). Carumonam was purchased from Takeda Pharmaceutical Co., Ltd. (Tokyo, Japan). [1-$^{13}$C]Hexanoic acid and [1,2,3,4-$^{13}$C]octanoic acid were purchased from Cambridge Isotope Laboratories, Inc. (Cambridge, MA, USA). All commercially available chemicals for chemical synthesis were used without further purification.

*Analytical Methods*—The $^{1}$H and $^{13}$C NMR spectra of **1** and CoA derivatives were recorded on JEOL JNM-ECA-500 and JNM-AL-400 spectrometers (JEOL, Ltd., Tokyo, Japan). Chemical shifts (in ppm) were referenced against the residual solvent for $^{1}$H NMR and TSP-d4 as an external standard for $^{13}$C NMR. UV absorbance was measured using a JASCO V-630 BIO spectrophotometer (JASCO Co., Tokyo, Japan). Fast atom bombardment (FAB) mass spectra were obtained using a JMS-700 mass spectrometer. Electrospray ionization (ESI) mass spectra of CoA-derivatives were obtained on a Bioapex-II Fourier transform ion cyclotron resonance mass spectrometer (Bruker Daltonics Japan, Ltd., Tokyo, Japan) and Synapt G2 (Waters, MA, USA). ESI-MS analysis of RM derivatives and RevS and RevT reaction products were performed using a Waters Alliance HPLC system equipped with a mass spectrometer (Q-TRAP, Applied Biosystems, CA, USA)

Matrix-assisted laser desorption/ionization-time-of-flight (MALDI-TOF)/mass spectrometry (MS) analysis of acyl-ACP was performed using ultrafleXtreme (Bruker Daltonics, Billerica, MA, USA). Sinapinic acid was used as a matrix.

All chemical syntheses were carried out under a nitrogen atmosphere and monitored by TLC with 0.25-mm pre-coated silica gel plates 60F254 Art 5715 (Merck, Darmstadt, Germany). Visualization was achieved using UV light and 10% ethanol solution of phosphomolybdic acid, followed by heating. For column chromatography, Silica Gel 60 N (spherical, neutral, 0.04–0.05 mm. Kanto Chemical Co, Inc., Tokyo, Japan) and Cosmosil 75C18-DNP (Nacalai Tesque Inc., Kyoto, Japan) were utilized.

*Bacterial Strains and Plasmids*—*Escherichia coli* DH5α (Takara Bio Inc., Shiga, Japan) and *E. coli* GM2929 *hsdS*::Tn10 carrying pUB307-aph::Tn7 were used for general DNA manipulation and *E. coli-Streptomyces* sp. SN-593 conjugation, respectively (39). *Escherichia coli* BL21 Star$^{TM}$ (DE3) (Invitrogen, Carlsbad, CA, USA) and *Streptomyces lividans* TK23 were to prepare the recombinant protein, and pET28b(+) (Novagen, Madison, WI, USA) and pWHM3 (40) were used as expression vectors, respectively.

*Culture Conditions*—*E. coli* strains were grown at 37°C in LB (1% Bacto-tryptone (BD Biosciences, Franklin Lakes, NJ, USA), 0.5% yeast extract (BD Biosciences), and 1% NaCl), LB agar Miller (Nacalai Tesque, Inc., Kyoto, Japan), or Terrific broth (TB) (1.2 % (w/v) Bacto-tryptone, 2.4% (w/v) yeast extract, 0.4% (v/v) glycerol, 0.231% (w/v) $KH_2PO_4$, and 1.254% (w/v) $K_2HPO_4$). To select for plasmid-containing cells, 100 μg ml$^{-1}$ ampicillin, 50 μg ml$^{-1}$ kanamycin, 30 μg ml$^{-1}$ chloramphenicol, 50 μg ml$^{-1}$ streptomycin, or 100 μg ml$^{-1}$ spectinomycin were added to an LB plate. *Streptomyces* sp. SN-593 culture conditions were described previously (38). *S. lividans* TK23 cells were cultured at 28°C in SK2 medium (1.4% (w/v) soluble starch, 0.35% (w/v) glucose, 0.35% (w/v) yeast extract, 0.21% (w/v) Bacto-peptone, 0.21% (w/v) beef extract (Remel Inc., KS, US), 0.014% (w/v) $KH_2PO_4$, and 0.042% (w/v) $MgSO_4$; pH 7.0).

*Plasmid Construction for Gene Disruption and Complementation*—The *revR*, *revS*, and *revT* gene disruption was performed by PCR-targeted gene replacement using the plasmids pKD46, pKD13, and pCP20 and *E. coli* BW25113 (41,42). Ampicillin-resistant pKD46 containing the λ Red-mediated recombination functions was used with the chloramphenicol-resistant pCC1FOS fosmid clone 3C11 containing the *revR*, *revS*, and *revT* genes. The plasmid pKD13 was used as a template for the FRT-flanked kanamycin-resistant gene cassette (42,43).

To construct the *revR*, *revS*, and *revT* gene replacement plasmids, DNA fragments containing the disrupted gene were amplified by PCR using PrimeSTAR®HS DNA polymerase (TaKaRa Bio). PCR conditions were as follows: 98°C for 10 sec, 25 cycles of 98°C for 10 sec, 62°C for 5 sec, and 68°C for 5 min. The amplified fragments were ligated to the HindIII site of the pIM vector (38). For Southern analysis (Fig. 2), the AlkPhos Direct Labelling and Detection System (GE Healthcare, Little Chalfont, UK) was used. The primers used for gene disruptions and Southern analysis are shown in Table 1.

To obtain the gene complementation plasmid, the *revR*, *revS*, and *revT* genes were ligated into the BamHI and HindIII sites of pTYM19 with *aphII* promoter (38,44). Because the *revR* gene includes a BamHI site in the sequence, a silent mutation was introduced using the QuikChange protocol (Stratagene, La Jolla, CA, USA). The *revR* gene inserted into the NdeI/XhoI restriction sites of the pET28b vector was amplified using *PfuTurbo* DNA polymerase (Stratagene) and the following primer pairs (with the mutation sites underlined): 5′-TCCAGCGACGAGTGGATACGCCGGCACTCCGGGAT-3′ and 5′-ATCCCGGAGTGCCGGCGTATCCACTCGTCGCTGGA-3′. PCR conditions were as follows: 98°C for 30 sec, 20 cycles of 98°C for 30 sec, 60°C for 1 min, and 68°C for 13 min. The resultant pET28b-*revR*-BamHI_mut vector was used as a template for the complementation plasmid (Table 1).

*Plasmid Construction for Heterologous Gene Expression in E. coli*—The *revS* (1740 bp) and *revT* (1332 bp) genes were amplified from the fosmid clone (PCC1FOS-3C11) using PrimeSTAR®HS DNA polymerase under the following conditions: 98°C for 10 sec and 25 cycles of 98°C for 10 sec, 62°C for 5 sec, and 68°C for 1.5 min. The *SRE2849* gene (243 bp) coding ACP of *Streptomyces* sp. SN-593 was amplified from PCC1FOS-4B1 under the following conditions: 98°C for 10 sec and 25 cycles of 98°C for 10 sec, 60°C for 5 sec, and 68°C for 25 sec. The *Bacillus subtilis* 168 phosphopantetheinyl transferase gene (*sfp*) (654 bp) was amplified from pUC19-*sfp* under the following conditions: 98°C for 10 sec and 25 cycles of 98°C for 10 sec, 62°C for 5 sec, and 68°C for 30 sec (45). The primers used for amplification are shown in Table 1. After restriction enzyme digestion, the *revS*, *revT*, *SRE2849*, *and sfp* gene fragments were inserted into the NdeI and XhoI sites of pET28b(+) or pACYCDuet-1 to construct pET28b-*revS*, pET28b-*revT*, pET28b-*SRE2849*, and pACYCDuet-1-*sfp*, respectively.

*Plasmid Construction for Heterologous Gene Expression in S. lividans TK23*—The β lactamase gene in the pWHM3 vector was replaced with the *aphI* gene using λRed recombination to form pWK. Next, the *tipA* promoter ($P_{tipA}$) was inserted into the EcoRI and BamHI sites to construct pWK-$P_{tipA}$ for expression in *S. lividans* TK23. To facilitate enzyme purification, the *revT* gene containing a His8-tag coding sequence was amplified from pET28b-*revT* using the primers shown in Table 1. After restriction enzyme digestion, the fragment was inserted into the BamHI and HindIII sites of pWK-$P_{tipA}$ to construct pWK-$P_{tipA}$-*revT*.

*Heterologous Gene Expression and Purification of Enzymes*—To obtain recombinant RevS, the expression plasmid was transformed into *E. coli* BL21 Star™ (DE3) cells. The resultant transformants were grown on LB medium containing 50 μg ml$^{-1}$ kanamycin overnight. To 200 ml TB containing 50 μg ml$^{-1}$ kanamycin, the preculture was added at an initial optical density of 0.1 at 600 nm ($OD_{600}$). Cells were cultured at 18°C. When the $OD_{600}$ reached 0.6, isopropyl β-D-1-thiogalactopyranoside was added to a final concentration of 0.5 mM. After further growth for 18 h at 18°C, the cells were harvested by centrifugation and frozen at –80°C.

After thawing on ice, the cells were suspended in 20 ml of extraction buffer (50 mM Tris-HCl, pH 7.5, 500 mM NaCl, and 20% glycerol, 5 mM imidazole, 0.5 mg ml$^{-1}$ lysozyme, and 6.25 U ml$^{-1}$ benzonase (Sigma-Aldrich)). For stabilization of recombinant RevS, octanoic acid was added to the cell suspension at a final concentration of 1 mM. The cell suspension was sonicated 10 times on ice for 10 sec with 1 min interval between each

sonication treatment (UD-200, TOMY, Tokyo, Japan). Cell debris was removed by centrifugation (10,000 ×*g* for 30 min) (SRX-201, TOMY), and then the supernatant was applied to a Ni-nitrilotriacetic acid (Ni-NTA) agarose (Qiagen, Hilden, Germany) column (2 × 4 cm) that had been equilibrated with buffer A (50 mM Tris-HCl, pH 7.5, 500 mM NaCl, and 20% glycerol) containing 5 mM imidazole. After washing with the same buffer, non-specifically bound proteins were removed by washing with 20 ml of buffer A containing 5 mM imidazole and 0.2% Tween 20. After removing Tween 20 with 40 ml of buffer A containing 5 mM imidazole, the column was further washed with 40 ml of buffer A containing 40 mM imidazole. The His-tag fusion protein was eluted with 25 ml of butter A containing 250 mM imidazole. The eluted fraction was concentrated using an Amicon Ultra centrifugal filter (Merck, Darmstadt, Germany), and the buffer was exchanged for stock buffer (50 mM Tris-HCl, pH 7.5, 200 mM NaCl, 20% glycerol) on the centrifugal filter. The purity of RevS was confirmed by SDS-PAGE. Size exclusion chromatography was performed as described previously (46).

To obtain recombinant RevT, pWK-$P_{tipA}$-*revT* was introduced into *S. lividans* TK23 using a polyethylene glycol-mediated protoplast method (47). The resulting transformants were grown in SK2 medium containing 15 μg $ml^{-1}$ kanamycin for 2 days, and then 1 ml preculture was inoculated into 70 ml of SK2 medium containing 15 μg $ml^{-1}$ kanamycin. After 1 day of culture, thiostrepton was added at a final concentration of 50 μg $ml^{-1}$ to express RevT. After another 1 day of culture, the cells were harvested by centrifugation and frozen at –80°C. Purification of RevT was performed as described for RevS. The His-tag fusion protein was eluted with 5 ml of butter A containing 250 mM imidazole and 1 mM NADPH and used for biochemical characterization. The purity of RevT was confirmed by SDS-PAGE. Size exclusion chromatography was performed using 50 mM Tris-HCl (pH 7.5), 10 mM $NaHCO_3$, 200 mM NaCl, and 10% glycerol.

To obtain apo-ACP, pET28b-*SRE2849* was transformed into *E. coli* BL21 Star™ (DE3) cells. The transformants were selected on LB medium containing 50 μg $ml^{-1}$ kanamycin. Heterologous expression and purification were performed as described for RevS. The fraction eluted from the Ni-NTA column was concentrated using an Amicon Ultra centrifugal filter, and the buffer was exchanged for stock buffer.

To obtain holo-ACP, pET28b-*SRE2849* and pACYCDuet-1-*sfp* were co-transformed into *E. coli* BL21 Star™ (DE3) cells. Transformants were selected on LB medium containing 50 μg $ml^{-1}$ kanamycin and 30 μg $ml^{-1}$ chloramphenicol. Heterologous gene expression, Ni-NTA column chromatography, and buffer exchange were performed as described for apo-ACP. To eliminate α-*N*-gluconoylated holo-ACP (48) from the Ni-NTA fraction, holo-ACP was further purified using a MonoQ 5/50 column (GE Healthcare) that had been pre-equilibrated with 50 mM Bis-Tris (pH 6.5) buffer containing 0.2 M NaCl and 20% glycerol. After loading the Ni-NTA fraction (42.2 mg), the column was washed with equilibration buffer for 30 min at a flow rate of 0.2 ml $min^{-1}$, and eluted with a linear gradient of 0.2–0.5 M NaCl for 60 min. Subsequently, 400 μl of the Mono Q fraction (5.7 mg) containing holo-ACP was collected based on MALDI-TOF/MS analysis and used in the FAAL assay for RevS.

*FACL Assay of RevS*—For HPLC analysis of the RevS reaction product, an enzyme reaction was performed in a final reaction volume of 100 μl containing 100 mM HEPES (pH 7.5), 20% glycerol, 10 mM $MgCl_2$, 5 mM TCEP, 0.5 mM fatty acid, 2 mM CoA, 3 mM ATP, and 1 μM RevS. After preincubation of the reaction mixture at 25°C for 3 min, the reaction was initiated by the addition of RevS and allowed to proceed for 60 min. The reaction was terminated by the rapid addition of 0.5 μl formic acid and then centrifuged at 15,000 ×*g* for 10 min at 4°C (Kubota 3700, Kubota Co., Tokyo, Japan) to remove the protein. The supernatant was subjected to liquid chromatography (LC)/ESI- MS (Table 2).

To determine the substrate specificity of RevS, we quantified fatty acyl-CoA formation by HPLC

and NADH oxidation using a spectrophotometer. Because the stoichiometry of the product amount in both assays was identical, we performed a spectrophotometric assay to determine the kinetic parameters of RevS (49). Assays were performed in a 1-ml quartz cuvette with a final volume of 200 μl containing 100 mM HEPES (pH 7.5), 20% glycerol, 10 mM $MgCl_2$, 5 mM TCEP, 0.05–3 mM fatty acid, 2 mM CoA, 3 mM ATP, 0.4 mM phosphoenol pyruvate, 0.4 mM NADH, 5 U myokinase, 4.5 U pyruvate kinase, 5.8 U lactate dehydrogenase, and 0.5–2.5 μM RevS. Substrate and RevS concentrations were varied as follows: 0.1–2 mM heptanoic acid with 2 μM RevS, 0.1–2 mM octanoic acid with 1 μM RevS, 0.2–2 mM nonanoic acid with 1 μM RevS, 0.1 to 2 mM decanoic acid with 2 μM RevS, 0.2–2.2 mM (*E*)-2-hexenoic acid with 2 μM RevS, 0.1–2.5 mM (*E*)-2-heptenoic acid with 2.5 μM RevS, 0.1–3 mM (*E*)-2-octenoic acid with 2 μM RevS, 0.2–2.5 mM (*E*)-2-nonenoic acid with 1 μM RevS, 0.05–3 mM (*E*)-2-decenoic acid with 2 μM RevS, 0.05–3 mM (*E*)-2-undecenoic acid with 2 μM RevS, 0.05–3 mM (*E*)-3-hexenoic acid with 1 μM RevS, 0.05–3 mM (*E*)-3-heptenoic acid with 1 μM RevS, 0.05–3 mM (*E*)-3-octenoic acid with 0.5 μM RevS, 0.05–3 mM (*E*)-3-nonenoic acid with 0.5 μM RevS, and 0.05–3 mM (*E*)-3-decenoic acid with 0.5 μM RevS. The cofactor concentration varied from 0.01–0.1 mM for ATP and from 0.02–1 mM for CoA. After preincubation of the reaction mixture at 25°C for 3 min, the reaction was initiated by adding RevS and the initial rate of oxidation of NADH at 340 nm was measured using a spectrophotometer. The kinetic constant was calculated by a nonlinear regression fit to the Michaelis–Menten equation using SigmaPlot11 (Table 3).

*Preparation of (E)-2-nonenoyl-ACP*—(*E*)-2-nonenoyl-ACP was prepared from a reaction containing 100 mM HEPES (pH 7.5), 20% glycerol, 10 mM $MgCl_2$, 5 mM TCEP, 0.5 mM (*E*)-2-nonenoic acid, 0.4 mM of holo-ACP, 3 mM ATP, and 5 μM RevS in a final volume of 80 μl. After preincubation at 25°C for 3 min, the reaction was initiated by the addition of RevS and incubation for 4 h. The reaction mixture (10 μl) was applied to Microcon Ultracel YM-10 (Millipore, MA, USA). After buffer exchange with 50 mM Tris-HCl (pH 7.5), the formation of (*E*)-2-nonenoyl-ACP was confirmed based on MALDI-TOF/MS analysis. The reaction mixture (70 μl) containing (*E*)-2-nonenoyl-ACP was used for RevT reaction.

*Enzyme Assay of RevT*—To detect the RevT reaction product, the assay were performed in a final volume of 100 μl containing 100 mM Tris-HCl (pH 7.5), 10% glycerol, 10 mM $NaHCO_3$, 11 mM $MgCl_2$, 1 mM EDTA, 0.5 mM (*E*)-2-enoyl-CoA, 4 mM NADPH, and 1 μM RevT. After preincubation of the reaction mixture at 25°C for 3 min, the reaction was initiated by the addition of RevT and allowed to proceed for 10–30 min. The reaction was terminated by the rapid addition of 0.5 μl formic acid and centrifuged at 15,000 ×*g* for 10 min at 4°C to remove the protein. The supernatant was subjected to LC/ESI-MS analysis.

To determine the kinetic parameters of RevT, we quantified both butylmalonyl-CoA formation by HPLC and NADPH oxidation using a spectrophotometer. Because the stoichiometry of the reaction product in both assays was identical, we conducted a spectrophotometric assay. The assay was performed in a 1-ml quartz cuvette in a final volume of 200 μl containing 100 mM Tris-HCl (pH 7.5), 10% glycerol, 10 mM $NaHCO_3$, 11 mM $MgCl_2$, 1 mM EDTA, 0.5 mM (*E*)-2-enoyl-CoA, 0.3 mM NADPH, and 1 μM RevT. NADPH concentration was varied from 0.01–0.3 mM. The substrate concentration for (*E*)-2-enoyl-CoA varied from 0.1–2 mM. After preincubation of the reaction mixture at 25°C for 3 min, the reaction was initiated by adding RevT, and NADPH oxidation at 340 nm was measured using a spectrophotometer. The kinetic constant was calculated by a nonlinear regression fit to the Michaelis–Menten equation using SigmaPlot11 (Table 4).

To examine the substrate specificity of RevT for (*E*)-2-enoyl-ACP, the reaction was performed in a final volume of 40 μl containing 100 mM Tris-HCl (pH 7.5), 10% glycerol, 10 mM $NaHCO_3$, 11 mM $MgCl_2$, 1 mM EDTA, 0.23 mM (*E*)-2-nonenoyl-ACP, 4 mM NADPH, and 5 μM RevT. After the

reaction was allowed to proceed at 25°C for 3 h, the reaction mixture (40 μl) was applied to Microcon Ultracel YM-10. After buffer exchange with 50 mM Tris-HCl (pH 7.5), the reaction product was analyzed by MALDI-TOF/MS.

*In Vitro Reconstruction of Butylmalonyl-CoA*—An enzyme coupling assay was performed for 1 h at 25°C in 100 mM Tris-HCl (pH 7.5) buffer containing 20% glycerol, 10 mM $NaHCO_3$, 11 mM $MgCl_2$, 1 mM EDTA, 5 mM TCEP, 0.5 mM (*E*)-2-hexenoic acid, 2 mM CoA, 3 mM ATP, 4 mM NADPH, 1 μM RevS, and 1 μM RevT in a final volume of 100μl. The reaction was terminated by the rapid addition of 0.5 μl formic acid and centrifuged at 15,000 ×*g* for 10 min at 4°C to remove the protein. The supernatant was subjected to LC/ESI-MS analysis.

*LC/ESI-MS Analysis of Enzyme Reaction Products*—To analyze of the reaction products of RevS, a LC/ESI-MS analysis was carried out. An Applied Biosystems Q-TRAP was connected to a Waters Alliance 2965 with a 2996 photodiode array detector and an XTerra®MS $C_{18}$ column (5 μm, 2.1 × 150 mm (Waters)). The HPLC conditions were as follows: 0.25 ml $min^{-1}$ flow rate; solvent A: water containing 40 mM ammonium acetate (pH 6.8); solvent B: acetonitrile. The conditions of the linear gradient elution were optimized to detect each RevS reaction product. The column was equilibrated with 2% solvent B. After injection of 1 μl of the sample into the equilibrated column, the column was developed using a linear gradient from 2–20% for saturated acyl-CoA, 2–50% for (*E*)-2-enoyl-CoA, and 2–65% acetonitrile for (*E*)-3-enoyl-CoA over 45 min. After the gradient, the column was washed with 100% solvent B for 10 min. All mass spectra were collected in the ESI-negative mode (Table 2).

To analyze the reaction products of RevT, LC/ESI-MS analysis was carried out. The HPLC conditions were as follows: 5 μm (2.1 × 150 mm) column, XTerra®MS $C_{18}$; 0.25 ml $min^{-1}$ flow rate; solvent A: water containing 40 mM ammonium acetate (pH 5); solvent B: acetonitrile. After injection of 1 μl sample into the column that had been equilibrated with 2% solvent B, the column was developed over a linear gradient of 2–25% solvent B for 30 min and washed with 100% solvent B for 10 min. Mass spectra were collected in the ESI-negative mode.

*Feeding of Labeled Precursors and Isolation of **1***—The Δ*revR* mutants were grown in 70 ml SY medium for 2 days at 28°C, and then 1 ml of the preculture was inoculated into 70 ml of PV8 medium. After 2 days of culture at 28°C, [1-$^{13}$C]hexanoic acid or [1,2,3,4-$^{13}$C]octanoic acid were added to the culture at a final concentration of 0.3 mM. Five days after inoculation, an equal volume of acetone was added to the broth and filtered to remove the mycelia. The filtrate was evaporated *in vacuo* to obtain an aqueous solution. The solution was adjusted to pH 4 using acetic acid and extracted twice with the same volume of ethyl acetate. The organic layer was dried over $Na_2SO_4$ and concentrated under reduced pressure to yield a brown oil. 1.5 g of extract from 2 L of [1-$^{13}$C]hexanoic acid feeding culture and 0.5 g of extract from 1 L of [1,2,3,4-$^{13}$C]octanoic acid feeding culture were obtained.

The 1.5 g extract from [1-$^{13}$C]hexanoic acid feeding was subjected to silica gel chromatography with stepwise-elution from 100:0 to 0:100 with $CHCl_3$–methanol. **1** was eluted 100:10 with $CHCl_3$-methanol. The fraction was separated using a Waters 600 HPLC system equipped with a 2996 photodiode array detector and a Senshu Pak Pegasil ODS column (20 × 250 mm) using an acetonitrile/0.05% aqueous formic acid isocratic system (48/52) at a flow rate of 9 ml $min^{-1}$ to yield 7.7 mg of **1**.

The 0.5 g extract from the [1,2,3,4-$^{13}$C]octanoic acid feeding was separated on a Sephadex LH-20 column (GE Healthcare) and eluted with methanol. The fractions containing **1** were applied to a 12-g Redi*Sep* Rf column (Teledyne Isco, Inc., Lincoln, NE, USA) for medium-pressure liquid chromatography with linear gradient from 20:80 to 100:0 of ethyl acetate-hexane for 35 min at a flow rate 30 ml $min^{-1}$ to obtain 28 fractions. The fraction containing **1** was separated on a Senshu Pak Pegasil ODS (10 × 250 mm) column using a

methanol/0.05% aqueous formic acid isocratic system (67/33) at a flow rate of 4 ml $min^{-1}$ to yield 1.6 mg of **1**.

*Preparation of Butylmalonyl-CoA*—Butylmalonyl-CoA was prepared using the transesterification method (50). To a stirred solution of butylmalonic acid (2.11 g, 13.2 mmol) and thiophenol (1.42 g, 12.8 mmol) in 100 ml of dry *N*,*N*-dimethylformamide (DMF), was added a solution of *N*,*N'*-dicyclohexylcarbodiimide (DCC) (3.20 g, 15.5 mmol) in 100 ml of DMF dropwise at 0°C. After stirring for 2 h at 0°C, the reaction was quenched with 50 ml of cold water and the mixture was acidified to pH 4 using 1 M HCl. The precipitated solid was filtered off and the filtrate was extracted 3 times with 200 ml of ether. The combined ether layers were dried over $Na_2SO_4$ and concentrated. The residue was purified by silica gel column chromatography (*n*-hexane/ethyl acetate; 1/1) to give monothiophenyl butylmalonate as a colorless solid (465 mg, 1.86 mmol, 14%). The Rf value was 0.1 (*n*-hexane/ethyl acetate; 8/3). $^1$H NMR (400 MHz, $CDCl_3$) 0.93 (t, *J* = 7.0 Hz, 3H) 1.39 (m, 4H), 2.01 (m, 2H), 3.70 (t, *J* = 7.6 Hz, 1H), 7.43 (m, 5H). HRMS (FAB) *m/z* calculated for $C_{13}H_{15}O_3S$ $[M-H]^-$, 251.0742; found: 251.0739. To a stirred solution of CoA (free form, 100 mg, 130.2 mmol) in 7.6 ml of 0.1 M $NaHCO_3$, was added monothiophenyl butylmalonate (164 mg, 651 mmol, 5eq) at 0°C, and then 0.2 M NaOH solution was slowly added to increase the pH to 8. After stirring overnight, the solution was acidified to pH 5 using approximately 2 ml of 0.2 M HCl. The mixture was fractionated with 5 ml of ether twice, and 5 ml of ethyl acetate to remove excess thiophenyl ester and thiophenol. The resulting aqueous phase was lyophilized and the residue (220 mg), after adjusting the pH to 7.4 with 0.1 M $NaHCO_3$ solution, was purified using Cosmosil column chromatography (gradient elution with water/methanol; methanol: 0–7.5%). A combined fraction was lyophilized to give butylmalonyl-CoA in amorphous powder (101 mg, 111 mmol, 85% yield based on free form). The Rf value was 0.3 (*n*-butanol/acetic acid/$H_2O$; 4/1/2). HRMS (ESI) *m/z* calculated for $C_{28}H_{42}N_7O_{19}P_3SNa_5^+$ $[M+Na]^+$, 1020.0952; found: 1020.0952, $C_{28}H_{43}N_7O_{19}P_3SNa_4^+$ $[M+Na]^+$, 998.1133; found: 998.1132. $^1$H NMR (500 MHz, $D_2O$) δ: 0.76 (s, 3H), 0.88 (t, *J* = 6.9 Hz, 3H), 0.91 (s, 3H), 1.30 (m, 4H), 1.84 (m, 2H), 2.46 (t, *J* = 6.9 Hz, 2H), 3.07 (m, 2H), 3.38 (m, 2H), 3.48 (m, 2H), 3.57 (m, 2H), 3.87 (dd, *J* = 9.8, 4.6 Hz, 1H), 4.04 (s, 1H), 4.27 (brs, 2H), 4.62 (brs, 1H), 6.21 (d, *J* = 6.9 Hz, 1H), 8.31 (s, 1H), 8.59 (s, 1H). $^{13}$C NMR (125 MHz, $D_2O$) δ: 16.00, 20.76, 23.75, 24.64, 30.88, 31.90, 31.92, 32.22, 32.31, 38.20, 38.28, 41.12, 41.19, 41.48, 66.98, 68.39, 68.42, 74.73, 74.78, 76.84, 76.84, 76.93, 76.93, 86.67, 86.73, 89.26, 121.52, 142.78, 152.31, 155.83, 158.56, 176.78, 177.59, 179.02, 203.85.

*Preparation of* (*E*)*-2-hexenoyl-CoA and* (*E*)*-2-octenoyl-CoA*—(*E*)-2-hexenoyl-CoA was also prepared using the transesterification method (50). To a stirred solution of (*E*)-2-hexenoic acid (1.14 g, 10 mmol), thiophenol (10 g, 9.0 mmol), and *N*, *N*-dimethyl-4-aminopyridine (20 mg) in 10 ml of dry methylene chloride, was added a solution of DCC (2.48 g, 12.0 mmol) in 5 ml of dry methylene chloride at 0°C. After stirring for 1 h at 0°C and then for 1 h at room temperature, the precipitated solid was filtered off and the organic layer was evaporated. The residue was purified using silica gel column chromatography (*n*-hexane/ethyl acetate, 10/1) to give thiophenyl (*E*)-2-hexenoate as an oil (1.54 g, 7.46 mmol, 74%). The Rf value was 0.3 (*n*-hexane/ethyl acetate; 5/1). $^1$H NMR (400 MHz, $CDCl_3$) δ: 0.98 (t, *J* = 7.2 Hz, 3H) 1.53 (tq, *J* = 7.2, 7.2 Hz, 1H), 2.22 (dtd, *J* = 7.2, 7.2, 1.2 Hz, 2H), 6.19 (dt, *J* = 15.6, 1.2 Hz, 1H), 6.99 (dt, *J* = 15.6, 7.2 Hz, 1H), 7.44 (m, 5H). To a stirred solution of CoA (free form, 50 mg, 65.1 mmol) in 3.8 ml of 0.1 M $NaHCO_3$ solution, was added the solution of thiophenyl (*E*)-2-hexenoate (67.2 mg, 325.5 mmol, 5 eq) in 3 ml of tetrahydrofuran at 0°C. After stirring overnight at 4°C, the reaction mixture was concentrated and fractionated with 5 ml of ether twice to remove excess thiophenyl ester and thiophenol. The resulting aqueous phase was lyophilized and the pH of the residue was adjusted to 7.4 using 0.1 M $NaHCO_3$ solution before charge. The residue was purified using Cosmosil column

chromatography (gradient solution with water/methanol; methanol: 0–12.5%). A combined fraction was lyophilized to give (*E*)-2-hexenoyl-CoA in amorphous powder (40 mg, 46.3 mmol, 71% yield based on free form). The Rf value was 0.3 (*n*-butanol/acetic acid/$H_2O$; 4/1/2). HRMS (ESI) *m/z* calculated for $C_{27}H_{41}N_7O_{17}P_3SNa_4^+$ $[M+Na]^+$, 952.1083; found: 952.1081, $C_{27}H_{42}N_7O_{17}P_3SNa_3^+$ $[M+Na]^+$, 930.1264; found: 930.1264. $^1$H NMR (500 MHz, $D_2O$) δ: 0.77 (s, 3H), 0.91 (t, *J* = 6.3 Hz, 3H), 0.91 (s, 3H), 1.48 (m, 2H), 2.20 (dq, *J* = 6.9, 1.7 Hz, 2H), 2.46 (t, *J* = 6.3 Hz, 2H), 3.07 (t, *J* = 6.3 Hz, 2H), 3.39 (t, *J* = 6.9 Hz, 2H), 3.47 (t, *J* = 6.9 Hz, 2H), 3.58 (dd, *J* = 9.8, 4.6 Hz, 1H), 3.86 (dd, *J* = 9.7, 4.6 Hz, 1H), 4.05 (s, 1H), 4.27 (m, 1H), 4.60 (brs, 1H), 6.21 (m, 2H), 6.98 (dt, *J* = 15.4, 6.9 Hz, 1H), 8.29 (s, 1H), 8.59 (s, 1H). $^{13}$C NMR (125 MHz, $D_2O$) δ: 15.78, 20.97, 23.43, 23.73, 30.66, 36.59, 38.59, 38.26, 38.30, 41.15, 41.21, 41.54, 68.64, 68.68, 74.69, 74.73, 76.52, 76.55, 76.96, 77.35, 86.97, 87.01, 89.43, 121.51, 130.75, 142.80, 151.50, 152.32, 155.80, 158.55, 176.86, 177.59, 196.77.

(*E*)-2-octenoyl-CoA was synthesized from (*E*)-2-octenoic acid using the mixed anhydride method (51-53). To a stirred solution of (*E*)-2-octenoic acid (92.6 mg, 651 mmol) and triethylamine (81.4 mg, 813 mmol, 1.25 eq) in 20 ml of dry ether, was added ethyl chloroformate (88.2 mg, 813 mmol, 1.25 eq) slowly at 0°C. After stirring for 12 h at room temperature under an argon atmosphere, the separated solid was filtered off and washed quickly with a small amount of dry ether. The whole solution containing an approximately 10-fold molar excess of CoA as a reactant (ether solution, 20 ml: 32.55 M) was stored at 0°C under argon.

To a stirred solution of CoA (free form, 50 mg, 65.1 mmol) in 4 ml of 0.05 M $Na_2CO_3$ solution, 3 ml of ethyl acetate and 3 ml of ethanol, an ether solution of 2 ml of 65.1 mmol crude ethyl 1-oxo-oct-2-en carbonate (*n*-hexane/ethyl acetate; 5/3; Rf = 0.3) was added dropwise at 0°C at pH 8.2. After stirring for 2 h at room temperature, the reaction mixture was evaporated under reduced pressure to remove the organic solvent, and the resulting aqueous phase was lyophilized. The residue, after adjusting the pH to 7.4 with 0.1 M $NaHCO_3$ solution before charge, was purified using Cosmosil column chromatography (gradient elution with water/methanol; methanol: 0–20%). A combined fraction was lyophilized to give (*E*)-2-octenoyl-CoA in amorphous powder (24 mg, 26.9 mmol, 41% yield based on free form). The Rf value was 0.3 (*n*-Butanol/ acetic acid/$H_2O$; 4/1/2). HRMS (ESI) *m/z* calculated for $C_{29}H_{45}N_7O_{17}P_3SNa_4^+$ $[M+Na]^+$, 980.1396; found: 980.1393, $C_{29}H_{46}N_7O_{17}P_3SNa_3^+$ $[M+Na]^+$, 958.1577; found: 958.1570. $^1$H NMR (500 MHz, $D_2O$) δ: 0.77 (s, 3H), 0.87 (t, *J* = 6.9 Hz, 3H), 0.91 (s, 3H), 1.29 (m, 4H), 1.45 (m, 2H), 2.21 (m, 2H), 2.46 (t, *J* = 6.9 Hz, 2H), 3.08 (t, *J* = 6.3 Hz, 2H), 3.39 (t, *J* = 6.3 Hz, 2H), 3.47 (t, *J* = 6.3 Hz, 2H), 3.58 (dd, *J* = 9.8, 5.2 Hz, 1H), 3.86 (dd, *J* = 9.8, 4.6 Hz, 1H), 4.05 (s, 1H), 4.26 (m, 2H), 4.60 (brs, 1H), 6.21 (m, 2H), 6.98 (dt, *J* = 15.4, 6.9 Hz, 1H), 8.29 (s, 1H), 8.59 (s, 1H). $^{13}$C NMR (125 MHz, $D_2O$) δ: 16.12, 20.98, 23.74, 24.60, 29.62, 30.66, 33.44, 34.48, 38.27, 38.31, 41.15, 41.22, 41.53, 68.63, 68.67, 74.69, 74.73, 76.51, 76.54, 76.96, 77.36, 77.38, 86.95, 86.99, 89.43, 121.50, 130.60, 142.79, 151.87, 152.30, 155.79, 158.53, 176.85, 177.58, 196.76.

## Results

*Disruption of RevR, RevS, and RevT Genes and Analysis of Metabolite Profiles* ─In the **1** gene cluster, the *revR*, *revS*, and *revT* genes were in the same transcriptional unit. Based on BLAST searching, *revT* gene belongs to the CCR homologs which are distributed in gene clusters producing polyketide compounds with atypical extender units (27-31). In addition to the *revT* gene, homologs of the *revR* and *revS* genes were also distributed in various polyketide gene clusters (Fig.1) (I, II, III, and IV). Therefore, to understand the role of *revR*, *revS*, and *revT* genes, we conducted gene disruptions (Figs. 2A, 2C, and 2E). After confirmation of gene disruption (Δ*revR*, Δ*revS*, Δ*revT*) by Southern hybridization (Fig. 2B, 2D, and 2F), the metabolite profile of each gene disruptant was analyzed by LC/ESI-MS (Fig. 3). In the wild-type strain, **1** was the major product among the RM-derivatives (Fig. 1A and 3A). Interestingly,

Δ*revR* mutants selectively decreased the production of **1** (Fig. 3B). Reintroduction of the *revR* gene under the control of the *aph* promoter restored **1** production to wild-type levels (Fig. 3C). Δ*revS* mutants showed an approximately 50% reduction of all RM-derivatives (Fig. 1A and 3D), and the phenotype was recovered by reintroduction of the *revS* gene (Fig. 3E), suggesting that RevS is involved in the formation of C18 alkyl residues in RM derivatives. Additionally, Δ*revT* mutants completely abolished the production of RMs (Fig. 3F), which was restored by complementation with the *revT* gene (Fig. 3G), indicating that RevT is essential for the production of RMs.

*Purification and Characterization of RevS*—Based on BLAST searching, RevS belongs to the uncharacterized adenylate-forming enzyme family. Together with the gene disruption phenotype (Fig. 3D and 3E), we hypothesized that RevS should function as an FACL or FAAL. We heterologously expressed His8-tagged RevS in *E. coli* and purified the protein to homogeneity using Ni-NTA column chromatography (Fig. 4A). Both monomeric (65 kDa) and dimeric (123 kDa) RevS were observed following gel filtration analysis (Fig. 4B). After gel filtration chromatography, we evaluated the specific activity of the monomeric and dimeric fractions. Based on the FACL assay, the specific activities of the monomer and dimer fractions of RevS were the same as that of the purified RevS before gel filtration (Fig. 4C). Therefore, the multimeric status of RevS on gel filtration chromatography was speculated to be the monomer-dimer equilibrium.

To examine FACL activity, purified RevS was incubated with various fatty acids in the presence of ATP and CoA and the reaction products were analyzed by LC/ESI-MS. RevS activated both saturated and unsaturated fatty acids with carbon chain lengths of C4–C11 into fatty acyl-CoAs (Table 2), but did not activate fatty acids with chain lengths of more than C13. Efficient acyl-CoA formation was observed when middle chain fatty acids (C8-C10) were used as the substrate. Moreover, to examine FAAL activity, we heterologously expressed holo-ACP in *E. coli* and purified the protein to homogeneity using Ni-NTA column chromatography (Fig. 4D). Because the His-tag was not attached in Sfp, only holo-ACP was purified using Ni-NTA column chromatography after co-expression of Sfp and ACP in *E. coli*. The holo-ACP was further purified by MonoQ column chromatography and its modification was confirmed by MALDI-TOF/MS analysis (Fig. 4E). Next, purified RevS was incubated with various fatty acids in the presence of ATP and holo-ACP. Although the FAAL and FACL activities of RevS showed the same substrate specificity, the specific activity of FAAL was significantly lower than that of FACL (Fig. 4F).

*Analysis of Kinetic Properties of FACL activity of RevS*—To determine the kinetic parameters of RevS for each substrate, we performed spectrophotometric assays. The RevS reaction apparently followed Michaelis-Menten kinetics. High catalytic efficiency was observed when middle chain fatty acids (C8-C10) were used for the RevS assay (Table 3). In addition, RevS accepted both saturated and unsaturated fatty acids as substrates with the same catalytic efficiency. We also calculated kinetic constants for ATP and CoA. The $K_m$ and $k_{cat}$ values for ATP were 0.039 ± 0.004 mM and 56.7 ± 2.2 $min^{-1}$, respectively, giving a catalytic efficiency of 1456 $min^{-1}$ $mM^{-1}$. The $K_m$ and $k_{cat}$ values of CoA were 0.05 ± 0.01 mM and 39.6 ± 0.8 $min^{-1}$, respectively, giving a catalytic efficiency of 861 $min^{-1}$ $mM^{-1}$. The kinetic parameters were comparable to those for other FACLs reported previously (Table 3).

*Phylogenetic Analysis of RevS*—To obtain insight into the molecular evolution of RevS, we performed phylogenetic analysis of the RevS using the amino acid sequences of FACL, FAAL, and a variety of CoA ligases (Fig. 5A). Consistent with the presence of an FAAL-specific insertion motif (Fig. 5B) (14), RevS was classified in an FAAL clade. However, biochemical analyses clearly demonstrated that RevS is an FACL. Interestingly, RevS homologs such as CinT and SamR0482 associated in the biosynthetic gene cluster of

cinnabaramide and stambomycin (Fig. 1B), respectively, were found in the same branch, suggesting that CinT and SamR0482 may be middle chain FACLs. These RevS homologs may have evolved from the FAAL family and were adapted for the production of fatty acyl-CoAs to efficiently convert them into 2-alkylmalonyl-CoAs for the PKS extender unit.

*Purification and Biochemical Characterization of RevT*—To determine the function of RevT, His8-tag RevT was heterologously expressed in *S. lividans* TK23 and purified using Ni-NTA column chromatography. The molecular mass of the RevT was estimated to be 48 kDa by SDS-PAGE (Fig. 6A) and 178 kDa by gel filtration chromatography (Fig. 6B), suggesting that RevT exists as a tetramer. Incubation of purified RevT in the presence of (*E*)-2-hexenoyl-CoA, $NaHCO_3$, and NADPH was performed for 30 min. The time-dependent production of butylmalonyl-CoA was observed for 20 min (Fig. 6C).

Because the understanding of substrate specificity and kinetic properties of RevT is important for the synthesis of polyketide compounds, we also characterized the kinetic parameters of (*E*)-2-hexenoyl-CoA and (*E*)-2-octenoyl-CoA. The reaction apparently followed Michaelis-Menten kinetics. RevT catalyzed both (*E*)-2-hexenoyl-CoA and (*E*)-2-octenoyl-CoA with the same catalytic efficiency. The $K_m$ and $k_{cat}$ values of (*E*)-2-hexenoyl-CoA for the formation of butylmalonyl-CoA were 0.33 ± 0.06 mM and 29.9 ± 1.7 $min^{-1}$, respectively, giving a catalytic efficiency of 91.4 $min^{-1}$ $mM^{-1}$. The $K_m$ and $k_{cat}$ values of (*E*)-2-octenoyl-CoA for the formation of hexylmalonyl-CoA were 0.33 ± 0.04 mM and 36.2 ± 1.3 $min^{-1}$, respectively, giving a catalytic efficiency of 109 $min^{-1}$ $mM^{-1}$. The kinetic parameters were also evaluated for NADPH in the presence of (*E*)-2-hexenoyl-CoA and (*E*)-2-octenoyl-CoA (Table 4). The kinetic efficiency of RevT for (*E*)-2-octenoyl-CoA was better than that of CinF (31). Catalytic efficiency of SalG was significantly higher than that of RevT (27).

*Incorporation of $^{13}$C Labeled Fatty Acids into **1***—Biochemical analysis indicated that RevS efficiently converted fatty acids into octanoyl-CoA, nonanoyl-CoA, and decanoyl-CoA, which contain longer carbon chain than physiological RevT substrates. Therefore, the β-oxidation of fatty acyl-CoAs is essential for producing truncated (*E*)-2-enoyl-CoAs for RevT substrates. To understand the biosynthetic process, we performed a feeding experiment using [1,2,3,4-$^{13}$C]octanoic acid. We hypothesized the activation of labeled fatty acid into [1,2,3,4-$^{13}$C]octanoyl-CoA by RevS, the generation of [1,2-$^{13}$C](*E*)-2-hexenoyl-CoA after β-oxidation process, and the conversion into [1,2-$^{13}$C]butylmalonyl-CoA by RevT, resulting in assembly into the structure of **1** (Fig. 7A). In this experiment, we used the Δ*revR* mutant for efficient incorporation of the fatty acid precursor into **1**, because the mutants showed low yields of **1** (Fig. 3B). After feeding of [1,2,3,4-$^{13}$C]octanoic acid, we isolated **1** and analyzed its $^{13}$C-NMR spectrum. In addition to the signals at 25.4 and 84.2 ppm assigned to C17 and C18 of **1**, respectively, significant C-C coupling was observed. Moreover, the coupling constants were nearly the same value ($J$ = 36 and 37 Hz) (Fig. 7B). These results suggest that octanoic acid was incorporated into **1** through the biosynthetic pathway predicted in Fig. 7A. We also tested whether [1-$^{13}$C]hexanoic acid is incorporated into **1** (Fig. 7C). After the feeding experiment, we purified **1** from the Δ*revR* mutant culture and its $^{13}$C-NMR spectrum was analyzed (Fig. 7D). A corresponding signal at 25.4 ppm assigned to C17 of **1** was highly enriched, suggesting that hexanoic acid is utilized for **1** biosynthesis.

*RevS and RevT Are Responsible for Butylmalonyl-CoA Biosynthesis*—Because of efficient incorporation of fatty acids into **1**, we also investigated the successive conversion of (*E*)-2-hexenoic acid into (*E*)-2-hexenoyl-CoA by RevS and the reductase/carboxylase reaction by RevT to give butylmalonyl-CoA (Fig. 8A). As expected, (*E*)-2-hexenoic acid was efficiently converted into butylmalonyl-CoA in the RevS-RevT coupling reaction (Fig. 8B). This is the first report of *in vitro* reconstruction of 2-alkylmalonyl-CoA using physiological enzymes derived from a secondary

metabolite gene cluster.

Moreover, we examined whether the biosynthetic route occurs from (*E*)-2-hexenoic acid to (*E*)-2-enoyl-ACP and then 2-alkylmalonyl-ACP (Fig. 8C). Because the FAAL activity of RevS was very low (Fig. 4F), we first purified the FAAL reaction product, (*E*)-2-nonenoyl-ACP, using MonoQ column chromatography. Using the purified (*E*)-2-nonenoyl-ACP fraction, we performed the RevT reaction under optimized condition (Fig. 6). However, we did not detect the conversion of (*E*)-2-nonenoyl-ACP into 2-heptylmalonyl-ACP (Fig. 8D), suggesting that RevS and RevT are responsible for the production of 2-alkylmalonyl-CoA but not 2-alkylmalonyl-ACP.

**Discussion**

In this study, we characterized the *revR*, *revS*, and *revT* genes, which are involved in 2-alkylmalonyl-CoA formation in RM biosynthesis. *revR* gene disruption demonstrated that RevR was involved in the selective production of butylmalonyl-CoA, which was consistent with the high production of **1** in wild-type culture (Fig. 3). RevR showed 55% amino acid identity to BenQ that is reported to be crucial for providing the hexanoate PKS starter unit for benastatin biosynthesis (54,55). In addition, it has been reported that KASIII is a determinant of the fatty acid priming unit producing straight or branched chain, as well as the even- or odd number chain (56,57). RevR is likely to select butyryl-CoA as a priming substrate to yield 3-oxo-hexanoyl-ACP. Next, the product may be converted into (*E*)-2-hexenoyl-ACP by β-keto processing enzymes (Fig. 1C). In this *de novo* fatty acid biosynthetic pathway, an unknown transacylase may be responsible for the conversion of (*E*)-2-hexenoyl-ACP into (*E*)-2-hexenoyl-CoA, as RevT did not accept (*E*)-2-enoyl-ACP as a substrate (Fig. 8D). *revS* gene disruption and complementation analysis indicated the non-essentiality of RevS for the biosynthesis of RMs (Fig. 3D and 3E). We speculate that RMs biosynthesis in Δ*revS* mutants was mainly supported by *de novo* fatty acid biosynthesis (Fig. 1C). Another possibility is the involvement of unidentified CoA ligase, which may support medium chain acyl-CoA formation. We found three genes showing 30–43% amino acid identity to RevS in the draft genome of *Streptomyces* sp. SN-593. Although three were not in the FACL clade of RevS (Fig. 5A), gene disruption and biochemical analysis will be essential for final conclusions.

Overall, structure of the class I adenylate-forming enzymes are composed of large N-terminal and small C-terminal domains connected by a flexible hinge region (9). Crystal structure analysis of FAAL28 (FadD28) from *M. tuberculosis* revealed that FAAL has a specific insertion motif containing 22 amino acids (Fig. 5B). The insertion motif modulates C-terminal domain movement and disrupts access of the acyl-AMP intermediate to the CoA binding motif (14). Amino acid alignments and phylogenetic analysis of adenylate-forming enzymes indicated that RevS belongs to the FAAL clade. Unexpectedly, biochemical analysis of RevS revealed FACL activity even in the presence of the FAAL-specific insertion motif (Fig. 5). Arora *et al.* also reported that deletion of the insertion motif found in FadD28 resulted in the conversion of FAAL activity into FACL activity (14), indicating that FAAL originally contains CoA in the binding pocket. Since phylogenetic analysis suggested that FAAL was derived from CoA ligase, the FACL activity of RevS may have re-evolved from the FAAL clade by generating access to the CoA binding pocket by optimizing the orientation of the N- and C-terminal domains. Interestingly, in contrast to RevS, FadD10, which does not possess the FAAL-specific insertion motif, from *M. tuberculosis* showed FAAL activity. This was explained by the orientation of its N-terminal and C-terminal domains, which are quite different from those of other adenylate-forming family members (58). Therefore, crystal structure analysis of RevS is essential for fully understanding its biosynthetic mechanism.

Metabolite profiling of *revS* gene disruptants (Fig. 2 and 3) and kinetic analysis of RevS (Fig. 4, Table 2 and 3) also suggested the presence of available free fatty acids (C6–C10) during the late stationary phase and the close relationship between

fatty acid metabolism and polyketide biosynthesis. *Streptomyces* typically utilizes *de novo*-synthesized fatty acids not only for building membrane phospholipids but also to accumulate neutral lipid storage compounds such as triacylglycerol (TAG) (59-61). TAG is one of important carbon sources for energy production and a precursor for secondary metabolism. A link between TAG degradation and actinorhodin production has been suggested (59). Because TAG found in *S. lividans* consists of fatty acids ranging from C14–C18 (59), the fatty acids derived from TAG degradation should mainly be utilized for the production of acetyl-CoA, but not as RevS substrates. Therefore, other mechanisms may generate medium chain fatty acids to support the RevS reaction. A possible mechanism is termination of fatty acid biosynthesis by chain length-specific acyl-ACP-thioesterase. Interestingly, it has been reported that the seed of *Cuphea palustris* possessed C8- and C14-specific acyl-ACP-thioesterases, *Cp* FatB1 and *CP* FatB2, respectively, which is consistent with the accumulation of middle chain fatty acids in the seed (62). However, we found no homologous gene in *Streptomyces* sp. SN-593. Additional detailed studies are needed to understand fatty acid homeostasis during secondary metabolite biosynthesis.

In summary, 2-alkylmalonyl-CoA biosynthesis was strongly supported by the functions of RevR and RevS. These enzymes effectively utilized *de novo* fatty acid biosynthesis and fatty acid degradation products, respectively. Decreased supply of atypical building blocks in the polyketide assembly line is critical for secondary metabolite biosynthesis. Therefore, the presence of RevR and RevS may be a backup system to ensure the production of atypical extender units. Our results explain why homologs of RevR and RevS are distributed in polyketide biosynthetic gene clusters, which utilize atypical extender units (Fig. 1).

*Acknowledgments—We thank Dr. K. Matsumoto for valuable advice and comments. We thank Dr. M. Uramoto for NMR analysis. We thank Dr. N. Doumae for MALDI-TOF/MS analysis. We thank Dr. T. Nakamura and Dr. Y. Hongo for HRMS analysis. We thank Dr. T. Kumano, E. Oowada, H. Takagi, and A. Okano for technical assistance.*

**Conflict of interest:** The authors declare that they have no conflicts of interest with the contents of this article.

**Author contributions:** Takeshi Miyazawa performed the genetic, biochemical, and feeding experiments, and wrote the paper. Shunji Takahashi designed all of the studies, constructed vectors, and wrote the paper. Akihiro Kawata examined the assay condition for RevS. Suresh Panthee supported the isolation of gene disruptants. Teruo Hayashi and Takeshi Shimizu synthesized butylmalonyl-CoA, (*E*)-2-hexenoyl-CoA, and (*E*)-2-octenoyl-CoA. Toshihiko Nogawa supported LC/MS and NMR analysis. Hiroyuki Osada integrated this research. All authors reviewed the results and approved the final version of the manuscript.

**REFERENCE**


1. Harvey, A. L., Edrada-Ebel, R., and Quinn, R. J. (2015) The re-emergence of natural products for drug discovery in the genomics era. *Nat Rev Drug Discov* **14**, 111-129
2. Dias, D. A., Urban, S., and Roessner, U. (2012) A historical overview of natural products in drug discovery. *Metabolites* **2**, 303-336
3. Wilkinson, B., and Micklefield, J. (2007) Mining and engineering natural-product biosynthetic pathways. *Nat Chem Biol* **3**, 379-386
4. Wong, F. T., and Khosla, C. (2012) Combinatorial biosynthesis of polyketides--a perspective. *Curr Opin Chem Biol* **16**, 117-123
5. Winter, J. M., and Tang, Y. (2012) Synthetic biological approaches to natural product biosynthesis. *Curr Opin Biotechnol* **23**, 736-743
6. Steenbergen, J. N., Alder, J., Thorne, G. M., and Tally, F. P. (2005) Daptomycin: a lipopeptide antibiotic for the treatment of serious Gram-positive infections. *J Antimicrob Chemother* **55**, 283-288
7. Nakamura, H., Hamer, H. A., Sirasani, G., and Balskus, E. P. (2012) Cylindrocyclophane biosynthesis involves functionalization of an unactivated carbon center. *J Am Chem Soc* **134**, 18518-18521
8. Marrakchi, H., Lanéelle, M. A., and Daffé, M. (2014) Mycolic acids: structures, biosynthesis, and beyond. *Chem Biol* **21**, 67-85
9. Schmelz, S., and Naismith, J. H. (2009) Adenylate-forming enzymes. *Curr Opin Struct Biol* **19**, 666-671
10. Trivedi, O. A., Arora, P., Sridharan, V., Tickoo, R., Mohanty, D., and Gokhale, R. S. (2004) Enzymic activation and transfer of fatty acids as acyl-adenylates in mycobacteria. *Nature* **428**, 441-445
11. Edwards, D. J., Marquez, B. L., Nogle, L. M., McPhail, K., Goeger, D. E., Roberts, M. A., and Gerwick, W. H. (2004) Structure and biosynthesis of the jamaicamides, new mixed polyketide-peptide neurotoxins from the marine cyanobacterium *Lyngbya majuscula*. *Chem Biol* **11**, 817-833
12. Hansen, D. B., Bumpus, S. B., Aron, Z. D., Kelleher, N. L., and Walsh, C. T. (2007) The loading module of mycosubtilin: an adenylation domain with fatty acid selectivity. *J Am Chem Soc* **129**, 6366-6367
13. Wittmann, M., Linne, U., Pohlmann, V., and Marahiel, M. A. (2008) Role of DptE and DptF in the lipidation reaction of daptomycin. *FEBS J* **275**, 5343-5354

14. Arora, P., Goyal, A., Natarajan, V. T., Rajakumara, E., Verma, P., Gupta, R., Yousuf, M., Trivedi, O. A., Mohanty, D., Tyagi, A., Sankaranarayanan, R., and Gokhale, R. S. (2009) Mechanistic and functional insights into fatty acid activation in *Mycobacterium tuberculosis*. *Nat Chem Biol* **5**, 166-173
15. Léger, M., Gavalda, S., Guillet, V., van der Rest, B., Slama, N., Montrozier, H., Mourey, L., Quémard, A., Daffé, M., and Marrakchi, H. (2009) The dual function of the *Mycobacterium tuberculosis* FadD32 required for mycolic acid biosynthesis. *Chem Biol* **16**, 510-519
16. Gavalda, S., Léger, M., van der Rest, B., Stella, A., Bardou, F., Montrozier, H., Chalut, C., Burlet-Schiltz, O., Marrakchi, H., Daffé, M., and Quémard, A. (2009) The Pks13/FadD32 crosstalk for the biosynthesis of mycolic acids in *Mycobacterium tuberculosis*. *J Biol Chem* **284**, 19255-19264
17. Hayashi, T., Kitamura, Y., Funa, N., Ohnishi, Y., and Horinouchi, S. (2011) Fatty acyl-AMP ligase involvement in the production of alkylresorcylic acid by a *Myxococcus xanthus* type III polyketide synthase. *Chembiochem* **12**, 2166-2176
18. Vats, A., Singh, A. K., Mukherjee, R., Chopra, T., Ravindran, M. S., Mohanty, D., Chatterji, D., Reyrat, J. M., and Gokhale, R. S. (2012) Retrobiosynthetic approach delineates the biosynthetic pathway and the structure of the acyl chain of mycobacterial glycopeptidolipids. *J Biol Chem* **287**, 30677-30687
19. Cacho, R. A., Jiang, W., Chooi, Y. H., Walsh, C. T., and Tang, Y. (2012) Identification and characterization of the echinocandin B biosynthetic gene cluster from *Emericella rugulosa* NRRL 11440. *J Am Chem Soc* **134**, 16781-16790
20. Mareš, J., Hájek, J., Urajová, P., Kopecký, J., and Hrouzek, P. (2014) A hybrid non-ribosomal peptide/polyketide synthetase containing fatty-acyl ligase (FAAL) synthesizes the ß-amino fatty acid lipopeptides puwainaphycins in the Cyanobacterium *Cylindrospermum alatosporum*. *PLoS One* **9**, e111904
21. Ross, C., Scherlach, K., Kloss, F., and Hertweck, C. (2014) The molecular basis of conjugated polyyne biosynthesis in phytopathogenic bacteria. *Angew Chem Int Ed Engl* **53**, 7794-7798
22. Black, P. N., and DiRusso, C. C. (2003) Transmembrane movement of exogenous long-chain fatty acids: proteins, enzymes, and vectorial esterification. *Microbiol Mol Biol Rev* **67**, 454-472
23. Black, P. N., and DiRusso, C. C. (2007) Yeast acyl-CoA synthetases at the crossroads of fatty acid metabolism and regulation. *Biochim Biophys Acta* **1771**, 286-298
24. Wilson, M. C., and Moore, B. S. (2012) Beyond ethylmalonyl-CoA: the functional role of crotonyl-CoA carboxylase/reductase homologs in expanding polyketide diversity. *Nat Prod Rep*

**29**, 72-86

25. Erb, T. J., Berg, I. A., Brecht, V., Müller, M., Fuchs, G., and Alber, B. E. (2007) Synthesis of C5-dicarboxylic acids from C2-units involving crotonyl-CoA carboxylase/reductase: the ethylmalonyl-CoA pathway. *Proc Natl Acad Sci U S A* **104**, 10631-10636
26. Erb, T. J., Brecht, V., Fuchs, G., Müller, M., and Alber, B. E. (2009) Carboxylation mechanism and stereochemistry of crotonyl-CoA carboxylase/reductase, a carboxylating enoyl-thioester reductase. *Proc Natl Acad Sci U S A* **106**, 8871-8876
27. Eustaquio, A. S., McGlinchey, R. P., Liu, Y., Hazzard, C., Beer, L. L., Florova, G., Alhamadsheh, M. M., Lechner, A., Kale, A. J., Kobayashi, Y., Reynolds, K. A., and Moore, B. S. (2009) Biosynthesis of the salinosporamide A polyketide synthase substrate chloroethylmalonyl-coenzyme A from S-adenosyl-L-methionine. *Proc Natl Acad Sci U S A* **106**, 12295-12300
28. Mo, S., Kim, D. H., Lee, J. H., Park, J. W., Basnet, D. B., Ban, Y. H., Yoo, Y. J., Chen, S. W., Park, S. R., Choi, E. A., Kim, E., Jin, Y. Y., Lee, S. K., Park, J. Y., Liu, Y., Lee, M. O., Lee, K. S., Kim, S. J., Kim, D., Park, B. C., Lee, S. G., Kwon, H. J., Suh, J. W., Moore, B. S., Lim, S. K., and Yoon, Y. J. (2011) Biosynthesis of the allylmalonyl-CoA extender unit for the FK506 polyketide synthase proceeds through a dedicated polyketide synthase and facilitates the mutasynthesis of analogues. *J Am Chem Soc* **133**, 976-985
29. Xu, Z., Ding, L., and Hertweck, C. (2011) A branched extender unit shared between two orthogonal polyketide pathways in an endophyte. *Angew Chem Int Ed Engl* **50**, 4667-4670
30. Laureti, L., Song, L., Huang, S., Corre, C., Leblond, P., Challis, G. L., and Aigle, B. (2011) Identification of a bioactive 51-membered macrolide complex by activation of a silent polyketide synthase in *Streptomyces ambofaciens*. *Proc Natl Acad Sci U S A* **108**, 6258-6263
31. Quade, N., Huo, L., Rachid, S., Heinz, D. W., and Müller, R. (2012) Unusual carbon fixation gives rise to diverse polyketide extender units. *Nat Chem Biol* **8**, 117-124
32. Lechner, A., Wilson, M. C., Ban, Y. H., Hwang, J. Y., Yoon, Y. J., and Moore, B. S. (2013) Designed biosynthesis of 36-methyl-FK506 by polyketide precursor pathway engineering. *ACS Synth Biol* **2**, 379-383
33. Osada, H., Koshino, H., Isono, K., Takahashi, H., and Kawanishi, G. (1991) Reveromycin A, a new antibiotic which inhibits the mitogenic activity of epidermal growth factor. *J Antibiot (Tokyo)* **44**, 259-261
34. Woo, J. T., Kawatani, M., Kato, M., Shinki, T., Yonezawa, T., Kanoh, N., Nakagawa, H., Takami, M., Lee, K. H., Stern, P. H., Nagai, K., and Osada, H. (2006) Reveromycin A, an agent for osteoporosis, inhibits bone resorption by inducing apoptosis specifically in osteoclasts. *Proc*

*Natl Acad Sci U S A* **103**, 4729-4734

35. Muguruma, H., Yano, S., Kakiuchi, S., Uehara, H., Kawatani, M., Osada, H., and Sone, S. (2005) Reveromycin A inhibits osteolytic bone metastasis of small-cell lung cancer cells, SBC-5, through an antiosteoclastic activity. *Clin Cancer Res* **11**, 8822-8828
36. Hiraoka, K., Zenmyo, M., Watari, K., Iguchi, H., Fotovati, A., Kimura, Y. N., Hosoi, F., Shoda, T., Nagata, K., Osada, H., Ono, M., and Kuwano, M. (2008) Inhibition of bone and muscle metastases of lung cancer cells by a decrease in the number of monocytes/macrophages. *Cancer Sci* **99**, 1595-1602
37. Yano, A., Tsutsumi, S., Soga, S., Lee, M. J., Trepel, J., Osada, H., and Neckers, L. (2008) Inhibition of Hsp90 activates osteoclast c-Src signaling and promotes growth of prostate carcinoma cells in bone. *Proc Natl Acad Sci U S A* **105**, 15541-15546
38. Takahashi, S., Toyoda, A., Sekiyama, Y., Takagi, H., Nogawa, T., Uramoto, M., Suzuki, R., Koshino, H., Kumano, T., Panthee, S., Dairi, T., Ishikawa, J., Ikeda, H., Sakaki, Y., and Osada, H. (2011) Reveromycin A biosynthesis uses RevG and RevJ for stereospecific spiroacetal formation. *Nat Chem Biol* **7**, 461-468
39. Komatsu, M., Uchiyama, T., Omura, S., Cane, D. E., and Ikeda, H. (2010) Genome-minimized *Streptomyces* host for the heterologous expression of secondary metabolism. *Proc Natl Acad Sci U S A* **107**, 2646-2651
40. Vara, J., Lewandowska-Skarbek, M., Wang, Y. G., Donadio, S., and Hutchinson, C. R. (1989) Cloning of genes governing the deoxysugar portion of the erythromycin biosynthesis pathway in *Saccharopolyspora erythraea* (*Streptomyces erythreus*). *J Bacteriol* **171**, 5872-5881
41. Gust, B., Challis, G. L., Fowler, K., Kieser, T., and Chater, K. F. (2003) PCR-targeted *Streptomyces* gene replacement identifies a protein domain needed for biosynthesis of the sesquiterpene soil odor geosmin. *Proc Natl Acad Sci U S A* **100**, 1541-1546
42. Datsenko, K. A., and Wanner, B. L. (2000) One-step inactivation of chromosomal genes in *Escherichia coli* K-12 using PCR products. *Proc Natl Acad Sci U S A* **97**, 6640-6645
43. Cherepanov, P. P., and Wackernagel, W. (1995) Gene disruption in *Escherichia coli*: $Tc^R$ and $Km^R$ cassettes with the option of Flp-catalyzed excision of the antibiotic-resistance determinant. *Gene* **158**, 9-14
44. Onaka, H., Taniguchi, S., Ikeda, H., Igarashi, Y., and Furumai, T. (2003) pTOYAMAcos, pTYM18, and pTYM19, actinomycete-*Escherichia coli* integrating vextors for heterologous gene expression. *J Antibiot (Tokyo)* **56**, 950-956
45. Quadri, L. E., Weinreb, P. H., Lei, M., Nakano, M. M., Zuber, P., and Walsh, C. T. (1998)

Characterization of Sfp, a *Bacillus subtilis* phosphopantetheinyl transferase for peptidyl carrier protein domains in peptide synthetases. *Biochemistry* **37**, 1585-1595

46. Takahashi, S., Takagi, H., Toyoda, A., Uramoto, M., Nogawa, T., Ueki, M., Sakaki, Y., and Osada, H. (2010) Biochemical characterization of a novel indole prenyltransferase from *Streptomyces* sp. SN-593. *J Bacteriol* **192**, 2839-2851
47. Kieser, T., Bibb, M. J., Buttner, M. J., Chater, K. F., and Hopwood, D. A. (2000) *Practical Streptomyces Genetics*, the John Innes Foundation, Norwich, UK
48. Geoghegan, K. F., Dixon, H. B., Rosner, P. J., Hoth, L. R., Lanzetti, A. J., Borzilleri, K. A., Marr, E. S., Pezzullo, L. H., Martin, L. B., LeMotte, P. K., McColl, A. S., Kamath, A. V., and Stroh, J. G. (1999) Spontaneous alpha-*N*-6-phosphogluconoylation of a "His tag" in *Escherichia coli*: the cause of extra mass of 258 or 178 Da in fusion proteins. *Anal Biochem* **267**, 169-184
49. Hosaka, K., Mishina, M., Tanaka, T., Kamiryo, T., and Numa, S. (1979) Acyl-coenzyme-A synthetase I from *Candida lipolytica*. Purification, properties and immunochemical studies. *Eur J Biochem* **93**, 197-203
50. Padmakumar, R., Gantla, S., and Banerjee, R. (1993) A rapid method for the synthesis of methylmalonyl-coenzyme A and other CoA-esters. *Anal Biochem* **214**, 318-320
51. Quémard, A., Sacchettini, J. C., Dessen, A., Vilcheze, C., Bittman, R., Jacobs, W. R., and Blanchard, J. S. (1995) Enzymatic characterization of the target for isoniazid in *Mycobacterium tuberculosis*. *Biochemistry* **34**, 8235-8241
52. Parikh, S., Moynihan, D. P., Xiao, G., and Tonge, P. J. (1999) Roles of tyrosine 158 and lysine 165 in the catalytic mechanism of InhA, the enoyl-ACP reductase from *Mycobacterium tuberculosis*. *Biochemistry* **38**, 13623-13634
53. He, X., Alian, A., Stroud, R., and Ortiz de Montellano, P. R. (2006) Pyrrolidine carboxamides as a novel class of inhibitors of enoyl acyl carrier protein reductase from *Mycobacterium tuberculosis*. *J Med Chem* **49**, 6308-6323
54. Xu, Z., Schenk, A., and Hertweck, C. (2007) Molecular analysis of the benastatin biosynthetic pathway and genetic engineering of altered fatty acid-polyketide hybrids. *J Am Chem Soc* **129**, 6022-6030
55. Xu, Z., Metsä-Ketelä, M., and Hertweck, C. (2009) Ketosynthase III as a gateway to engineering the biosynthesis of antitumoral benastatin derivatives. *J Biotechnol* **140**, 107-113
56. Tsay, J. T., Oh, W., Larson, T. J., Jackowski, S., and Rock, C. O. (1992) Isolation and characterization of the beta-ketoacyl-acyl carrier protein synthase III gene (*fabH*) from *Escherichia coli* K-12. *J Biol Chem* **267**, 6807-6814

57. Rock, C. O., and Jackowski, S. (2002) Forty years of bacterial fatty acid synthesis. *Biochem Biophys Res Commun* **292**, 1155-1166

58. Liu, Z., Ioerger, T. R., Wang, F., and Sacchettini, J. C. (2013) Structures of *Mycobacterium tuberculosis* FadD10 protein reveal a new type of adenylate-forming enzyme. *J Biol Chem* **288**, 18473-18483

59. Olukoshi, E. R., and Packter, N. M. (1994) Importance of stored triacylglycerols in *Streptomyces*: possible carbon source for antibiotics. *Microbiology* **140**, 931-943

60. Arabolaza, A., Rodriguez, E., Altabe, S., Alvarez, H., and Gramajo, H. (2008) Multiple pathways for triacylglycerol biosynthesis in *Streptomyces coelicolor*. *Appl Environ Microbiol* **74**, 2573-2582

61. Gago, G., Diacovich, L., Arabolaza, A., Tsai, S. C., and Gramajo, H. (2011) Fatty acid biosynthesis in actinomycetes. *FEMS Microbiol Rev* **35**, 475-497

62. Dehesh, K., Edwards, P., Hayes, T., Cranmer, A. M., and Fillatti, J. (1996) Two novel thioesterases are key determinants of the bimodal distribution of acyl chain length of *Cuphea palustris* seed oil. *Plant Physiol* **110**, 203-210

63. Thompson, J. D., Higgins, D. G., and Gibson, T. J. (1994) CLUSTAL W: improving the sensitivity of progressive multiple sequence alignment through sequence weighting, position-specific gap penalties and weight matrix choice. *Nucleic Acids Res* **22**, 4673-4680

64. Zhang, Z., Zhou, R., Sauder, J. M., Tonge, P. J., Burley, S. K., and Swaminathan, S. (2011) Structural and functional studies of fatty acyl adenylate ligases from *E. coli* and *L. pneumophila*. *J Mol Biol* **406**, 313-324

65. Morsczeck, C., Berger, S., and Plum, G. (2001) The macrophage-induced gene (mig) of *Mycobacterium avium* encodes a medium-chain acyl-coenzyme A synthetase. *Biochim Biophys Acta* **1521**, 59-65

66. Khare, G., Gupta, V., Gupta, R. K., Gupta, R., Bhat, R., and Tyagi, A. K. (2009) Dissecting the role of critical residues and substrate preference of a Fatty Acyl-CoA Synthetase (FadD13) of *Mycobacterium tuberculosis*. *PLoS One* **4**, e8387

67. Chang, C., Huang, R., Yan, Y., Ma, H., Dai, Z., Zhang, B., Deng, Z., Liu, W., and Qu, X. (2015) Uncovering the Formation and Selection of Benzylmalonyl-CoA from the Biosynthesis of Splenocin and Enterocin Reveals a Versatile Way to Introduce Amino Acids into Polyketide Carbon Scaffolds. *J Am Chem Soc* **137**, 4183-4190

**FOOTNOTES**

*This work was partially supported by the JSPS KAKENHI Grant 24380052 and by a grant for "Project focused on developing key technology of discovering and manufacturing drug for next-generation treatment and diagnosis" from the Ministry of Economy, Trade and Industry (METI), Japan.

[1]To whom correspondence may be addressed: RIKEN Center for Sustainable Resource Science, Chemical Biology Group, Saitama 351-0198, Japan, Tel.: +81-48-467-4044; Fax: +81-48-462-4669; E-mail: shunjitaka@riken.jp, hisyo@riken.jp

[2]The abbreviations used are: ACP, acyl carrier protein; CCR, crotonyl-CoA carboxylase/reductase; LC/ESI-MS, liquid chromatography/electrospray ionization mass spectrometry; FAAL, fatty acyl-AMP ligase; FACL, fatty acyl-CoA ligase; NRPS, nonribosomal peptide synthetase; PKS, polyketide synthase; RM, reveromycin

FIGURE 1. **Biosynthetic genes responsible for polyketide extender units of RM-A.** *A*, Polyketide natural products containing atypical extender units. Bold in red indicates carbon chains derived from atypical extender units. *B*, Gene organization. Based on the presence of the *revR*, *revS*, and *revT* homologs, each gene cluster was categorized into four groups, including: *revR*, *revS*, and *revT* homologs (I), *revR* and *revT* homologs (II), *revT* homolog with additional genes related to atypical extender unit biosynthesis (III), and *revS* homolog with putative propionyl-CoA carboxylase β-subunit homolog (IV). *C*, The scheme of the possible 2-alkylmalonyl-CoA biosynthesis by RevR, RevS, and RevT. Both fatty acid degradation and *de novo* fatty acid biosynthetic pathway were predicted to be involved in 2-alkylmalonyl-CoA biosynthesis.

FIGURE 2. **Gene disruption and Southern hybridization.** *A*, scheme of *revR* gene disruption and restriction enzyme map of wild-type and Δ*revR* gene mutant strains. The bar shows the expected fragment size (bp) following NcoI and SalI digestion of genomic DNA. The bold bar shows the 3608-bp probe. *B*, Southern hybridization of genomic DNA from wild-type and *revR* gene disruptants. *C*, scheme of *rev*S gene disruption and a restriction enzyme map of wild-type and Δ*revS* gene mutant strains. The bar shows the expected fragment size (bp) after ApaLI and BalI digestion of genomic DNA. The bold bar shows the 5180-bp probe. *D*, Southern hybridization of genomic DNA from wild-type and *revS* gene disruptant. *E*, scheme of *revT* gene disruption and restriction enzyme map of wild-type and Δ*revT* gene mutant strains. The bar shows the expected fragment size (bp) following EcoRI and NotI digestion of genomic DNA. The bold bar shows 5399-bp probe. *F*, Southern hybridization of genomic DNA from wild-type and *revT* gene disruptant. Closed and open triangles show DNA fragments from wild-type and mutant strains, respectively.

FIGURE 3. **Metabolite profiles of gene disruptants.** HPLC analysis of ethyl acetate extract from wild-type strain (*A*), Δ*revR* mutant (*B*), and Δ*revR* mutant complemented with *revR* gene (*C*). Δ*revS* mutant (*D*) and Δ*revS* mutant complemented with *revS* gene (*E*). Δ*revT* mutant (*F*) and Δ*revT* mutant complemented with *revT* gene (*G*). **1–4** indicate RM-A, RM-C, RM-D, and RM-E, respectively. Asterisk indicates the peak of RM-B, which was non-enzymatically converted into 5,6-spiroacetal structure from **1** (38).

FIGURE 4. **Evaluation of FACL and FAAL activity of RevS.** *A*, SDS-PAGE analysis of RevS using 12.5% polyacrylamide gel. Lane 1, molecular mass markers; lane 2, purified RevS (1 μg). *B*, size exclusion chromatography of RevS. Purified protein (0.8 mg) was analyzed on a Superdex 200 column. *C*, Analysis of specific activity of the RevS fractions after gel filtration. The purified RevS after Ni-NTA column chromatography was fractionated by Superdex 200 chromatography (46). Two main peaks corresponding to the monomer and dimer fractions (each 4 ml) were concentrated using an Amicon Ultra centrifugal filter. In the presence of 1 μM RevS, 1 mM of octanoic acid, and 2 mM CoA, the specific activity was calculated using the spectrophotometric assay described in the Experimental procedures. Lane 1, purified RevS before gel filtration; lane 2, monomer fraction of RevS after gel filtration; lane 3, dimer fraction of RevS after gel filtration. *D*, SDS-PAGE analysis of purified apo- and holo-ACP using 15% polyacrylamide gel. Lanes 1 and 4, molecular mass markers; lane 2, His8-tag purified apo-ACP (1 μg); lane 3, His8-tag purified holo-ACP (1 μg). *E*, MALDI-TOF/MS analysis of apo-ACP (i), and holo-ACP and α-*N*-gluconoylated holo-ACP fraction after Ni-NTA column chromatography (ii), purified holo-ACP after removing α-*N*-gluconoylated holo-ACP by MonoQ column chromatography (iii). *F*, FACL (open bar) and FAAL (closed bar) activity of RevS were measured using an enzyme-coupled spectrophotometric assay. 0.3 mM of CoA or 0.3 mM of the purified holo-ACP was used to calculate specific activity of RevS.

FIGURE 5**. Phylogenetic analysis and multiple sequence alignments of RevS.**
*A*, Phylogenetic analysis of functionally annotated FACL, FAAL, and CoA ligases. Multiple sequence aliments were performed using the bootstrap method of CLASTALW (63). The bootstrap tree was drawn

using the neighbor-joining method in MEGA, version 6.06 (www.megasoftware.net). *B*, sequence aliments of RevS with FACL and FAAL, whose crystal structures have been solved. The bold bar shows FAAL-specific insertion motif (14,64).

Accession numbers used are as follows: Mav_Mig (AAB87139) from *Mycobacterium avium*; Ath At4g05160 (Q9M0X9), Ath ACOS5 (AAP03019.1), Ath 4-coumarate-CoA ligase 1 (AAD47191), Ath 4-coumarate-CoA ligase 2 (AAD47192), Ath 4-coumarate-CoA ligase 3 (AAD47194), and Ath 4-coumarate-CoA ligase 4 (Q9LU36) from *Arabidopsis thaliana*; Sce Faa1p (P30624) and Sce Faa3p (P39002) from *Saccharomyces cerevisiae* S288c, Rno FACL ACS1 (NP_036952), Rno ACS4 (NP_446075), Rno ACS5 (NP_446059), Rno ACS6_v1 (P33124), Rno FATP1 (Q60714) and Rno FATP4 (Q91VE0) from *Rattus norvegicus*; Eco FAAL (3PBK) (64), Eco FadD (AAA23752), Eco 2-amino-3-ketobutyryl-CoA ligase (1FC4_A), and Eco crotonobetaine/carnitine CoA ligase CaiC (CAA52113) from *E. coli*; Hsa Sa protein (BAB68363) from *Homo sapiens*; Rrh FadD19 (ADP09625) from *Rhodococcus rhodochrous*; Sam samR0482 (CAJ88192) from *Streptomyces ambofaciens* ATCC 23877 (30); Ssp CinT (CBW54660) from *Streptomyces* sp. JS360 (31); Tth FACL (Q5SKN9) from *Thermus thermophilus* Hb8; Tth phenylacetyl-CoA ligase (YP_004577) from *Thermus thermophilus* HB27; Mxa FtpD (YP_634753) from *Myxococcus xanthus* DK 1622 (17); Bxe benzoyl-CoA ligase (2V7B) from *Burkholderia xenovorans* Lb400; Bce phenylacetyl-CoA ligase Paak1 (2Y27_A) from *Burkholderia cenocepacia*; Awo caffeyl-CoA synthetase CarB (ADX43862) from *Acetobacterium woodii*; Bce *o*-succinylbenzyl-CoA ligase (ADK07438) from *Bacillus cereus* biovar anthracis str. CI; Mtu FadD3 (NP_218078.), Mtu FadD5 (NP_214680), Mtu FadD13 (NP_217605) (58), Mtu FadD15 (NP_216703), Mtu FadD19 (YP_177983), Mtu FadD10 (NP_214613), Mtu FadD28 (NP_217457) (18), Mtu FadD29 (NP_217466), Mtu FadD30 (NP_214918), Mtu FadD32 (NP_218318) (16), Mtu FadD33 (NP_215861), and Mtu FadD34 (YP_177686) from *Mycobacterium tuberculosis* H37Rv; Ssp RevS (BAK64635) from *Streptomyces* sp. SN-593, Lma JamA (AAS98774) from *Lyngbya majuscule* (11); Kse KSE_65520 (YP_004908267) from *Kitasatospora setae* KM-6054; Cal PuwC (AIW82280) from *Cylindrospermum alatosporum* CCALA 988 (20); Sro DptE (AAX31555) from *Streptomyces roseosporus* NRRL 11379 (13); Bgl CayA (AIG53815) from *Burkholderia gladioli* pv. *agaricicola* (21); Ssp salicylyl-CoA ligase (BAC78380) from *Streptomyces* sp. WA46; Sma benzoyl-CoA ligase (AAF81733) from *Streptomyces maritimus*; Bsu YhfL (NP_388908) from *Bacillus subtilis* subsp. subtilis str. 168; Lpn FAAL (3KXW) from *Legionella pneumophila* (64); Set FACL (1PG4) from *Salmonella enterica*.

FIGURE 6. **Biochemical characterization of RevT.** *A*, SDS-PAGE analysis of RevT using 12.5% polyacrylamide gel. Lane 1, molecular mass markers; lane 2, His8-tag purified RevT (1 μg). *B*, size exclusion chromatography of RevT. Purified protein (0.3 mg) was analyzed on a Superdex 200 column. *C*, LC/ESI-MS analysis of RevT reaction products. Synthetic standard of butylmalonyl-CoA (i), synthetic standard of (*E*)-2-hexenoyl-CoA (ii), and time-dependent production of butylmalonyl-CoA after 10 min (iii), 20 min (iv), and 30 min incubation (v). After heat treatment of RevT at 95°C for 5 min, the supernatant was collected by centrifugation at 15,000 ×*g* for 30 min at 4°C. Heat-treated RevT was incubated for 20 min (vi).

FIGURE 7. **Feeding of labeled fatty acid and $^{13}$C-NMR analysis.** *A*, Biosynthetic scheme of octanoic acid incorporation into **1**. *B*, $^{13}$C-NMR analysis of non-labeled **1** (i, iii) and labeled **1** after feeding of [1,2,3,4-$^{13}$C]octanoic acid (ii, iv). *C*, Biosynthetic scheme of hexanoic acid incorporation into **1**. *D*, $^{13}$C-NMR analysis of non-labeled **1** (i) and labeled **1** after feeding of [1-$^{13}$C]hexanoic acid (ii).

FIGURE 8. ***In vitro* enzyme coupling assay.** *A*, Reaction scheme of (*E*)-2-hexenoic acid into butylmalonyl-CoA by RevS and RevT. *B*, LC/ESI-MS chromatogram of butylmalonyl-CoA (i), (*E*)-2-hexenoic acid (ii),

1 h reaction product by RevS and RevT (iii), and 1 h reaction product using RevS and RevT treated at 95°C for 5 min (iv). Peaks corresponding to butylmalonyl-CoA and (*E*)-2-hexenoic acid were shown at 257 nm (blue line) and 240 nm (yellow line), respectively. *C*, Scheme of RevS and RevT reaction using ACP. *D*, Analysis of RevT reaction product by MALDI-TOF/MS. After RevS reaction using (*E*)-2-nonenoic acid and holo-ACP, the formation of (*E*)-2-nonenoyl-ACP was confirmed by MALDI-TOF/MS (i). The RevS reaction mixture containing (*E*)-2-nonenoyl-ACP was further reacted in the presence and absence of RevT (ii, iii).

**TABLE 1**
**Primers used in this study**

| **Primers used for the target gene inactivation by λ-Red system** | |
|---|---|
| Target gene (template DNA) | Primers |
| *revR* (pKD13) | *revR*-For-P4: 5′-GACGAGTGGATCCGCCGGCACTCCGGGATCGTCTCGCGC ATTCCGGGGATCCGTCGACC-3′ |
| | *revR*-Rev-P1: 5′ -TTCCATCGCCAGCGGGATGGAGGCGGCCGAGGTGTTGCC TGTAGGCTGGAGCTGCTTC-3′ |
| *revS* (pKD13) | *revS*-For-P4: 5′-GCCGACGACGCGGGCGCGAAGACGATCCTCACCACGACC ATTCCGGGGATCCGTCGACC-3′ |
| | *revS*-Rev-P1: 5′-GTAGAAGTTGCGGCCCTGGTGGATGACCACGTCCTTCAG TGTAGGCTGGAGCTGCTTC-3′ |
| *revT* (pKD13) | *revT*-For-P4: 5′-ACCGTGTGGTCGGCGATGTTCGAGCCCATCTCGACCTTC ATTCCGGGGATCCGTCGACC-3′ |
| | *revT*-Rev-P1: 5′ -TTACACGGACCGGAGCGGGTTGAGCTTCTGCTCACCCAG TGTAGGCTGGAGCTGCTTC-3′ |
| β-lactamase gene in pWHM3 (pKD13) | pKD13-*aphII*-For: 5′ -ATGAGTATTCAACATTTCCGTGTCGCCCTTATTCCCTTT AGAGCGCTTTTGAAGCTCA-3′ |
| | pKD13-*aphII*-Rev: 5′ -TTACCAATGCTTAATCAGTGAGGCACCTATCTCAGCGA GGAACTTCGGAATAGGAACT-3′ |
| **Primers used for DNA amplification, including target genes for disruption** | |
| Target gene (template DNA) | Primers |
| *revR and revS* (PCC1FOS-3C11) | Δ*revR/S*-HindIII-For: 5′-CCCAAGCTTGCCCGACCGGTACAGCGCGACCAT-3′ |
| | Δ*revR/S*-HindIII-Rev: 5′-CCCAAGCTTCCGAGGCGACCAGGTGCCACAGGT-3′ |
| *revT* (PCC1FOS-3C11) | Δ*revT*-HindIII-For: 5′-CCCAAGCTTCCAGCGCCACCATCATGGTGAAGA-3′ |
| | Δ*revT*-HindIII-Rev: 5′ -CCCAAGCTTGCAGTTCCAACCACGAACCGGAGT-3′ |
| **Primers used for heterologous expression in *E. coli*** | |
| Target gene (template DNA) | |

| | |
|---|---|
| *revR* (PCC1FOS-3C11) | *revR*-NdeI-For: 5′-GGAATTCCATATGGCGGGCACGATCGGCACGGCC-3′<br>*revR*-XhoI-Rev: 5′-CCGCTCGAGTCAGGGCAGGGCGACCACCATCGC-3′ |
| *revS* (PCC1FOS-3C11) | *revS*-NdeI-For: 5′-GGAATTCCATATGGAACTCGCCCTGCCGGCCGAG-3′<br>*revS*-XhoI-Rev: 5′-CCGCTCGAGTCACGCCTCCCGCGCCGGTGCC-3′ |
| *revT* (PCC1FOS-3C11) | *revT*-NdeI-For: 5′-GGAATTCCATATGGAACCCATGACCGAGGCAGTG-3′<br>*revT*-XhoI-Rev: 5′-CCGCTCGAGTTACACGGACCGGAGCGGGTTGAG-3′ |
| *acp* (PCC1FOS-4B1) | ACP-NdeI-For: 5′-GGAATTCCATATGGCCACCAAGGAAGAGATCGTC-3′<br>ACP-XhoI-Rev: 5′-CCGCTCGAGTCAGCCCTGTGCCTTGAGGATGTA-3′ |
| *sfp* (pUC19-*sfp*) | *sfp*-NdeI-For: 5′-CGAATTCCATATGAAGATTTACGGAATTTA-3′<br>*sfp*-XhoI-Rev: 5′-CCGCTCGAGTTATAAAAGCTCTTCGT-3′ |

**Primers used for pTYM19 complementation vector**

| Target gene (template DNA) | Primers |
|---|---|
| *revR* (pET28b-*revR*-BamHI_mut) (1002 bp) | *revR*-BamHI-For: 5′-CGCGGATCCATGGCGGGCACGATCGGCACG-3′<br>*revR*-HindIII-Rev: 5′-CCCAAGCTTTCAGGGCAGGGCGACCACCATC-3′ |
| *revS* (PCC1FOS-3C11) (1740 bp) | *revS*-BamHI-For: 5′-CGCGGATCCATGGAACTCGCCCTGCCGGCC-3′<br>*revS*-HindIII-Rev: 5′ -CCCAAGCTTTCACGCCTCCCGCGCCGGTGC-3′ |
| *revT* (PCC1FOS-3C11) (1332 bp) | *revT*-BamHI-For: 5′-CGCGGATCCATGGAACCCATGACCGAGGCAGTG-3′<br>*revT*-HindIII-Rev: 5′-CCCAAGCTTTTACACGGACCGGAGCGGGTTGAG-3′ |

**List of primer used for Southern blot analysis**

| Target gene (template) | Primers | Probe (bp) | Enzyme | Fragment size (bp) | |
|---|---|---|---|---|---|
| | | | | Wild-type | mutant |
| Δ*revR* (pIM-Δ*revR*) | *revR*-probe-For: 5′-CCCGAACCGCGAGTAACGCCAGTA-3′<br>*revR*-probe-Rev: 5′-GATCCTCACCACGACCGCCGTCAA-3′ | 3608 | NcoI | 10808 | 2889<br>8520 |
| | | | SalI | 849<br>4509 | 2070<br>3889 |
| Δ*revS* (pIM-Δ*revS*) | *revS*-probe-For: 5′-CCCAAGCTTGCCCGACCGGTACAGCG CGACCAT-3′ | 5180 | ApaLI | 542<br>1495<br>2332<br>7279 | 542<br>1495<br>2332<br>6361 |

| | | | | | |
|---|---|---|---|---|---|
| | *revS*-probe-Rev: 5′-CCCAAGCTTCCGAGGCGACCAGGTGC CACAGGT-3′ | | BalI | 2615<br>6246 | 2615<br>5328 |
| Δ*revT* (pIM-Δ*revT*) | *revT*-probe-For: 5′-CCCAAGCTTCCAGCGCCACCATCA TGGTGAAGA-3′ | 5399 | EcoRI | 4498<br>16321 | 3565<br>16321 |
| | *revT*-probe-Rev: 5′-CCCAAGCTTGCAGTTCCAACCACG AACCGGAGT-3′ | | NotI | 5109<br>8754 | 4176<br>8754 |

Underlines (6–14-bp and 39-bp) show restriction enzyme sites and homologous sequences to the target DNA region, respectively.

**TABLE 2**
**Summary of RevS reaction products**
RevS reaction products were analyzed by LC/ESI-MS as described in the Experimental procedures. All mass spectra were collected in the ESI-negative mode.

| Substrates | RevS reaction product | | |
|---|---|---|---|
| | Retention time (min) | *m/z* $[M-H]^-$ | Structure of product speculated |
| butanoic acid[a] | 17.6 | 836 | 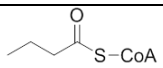 |
| pentanoic acid[a] | 21.1 | 850 | 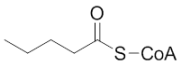 |
| hexanoic acid[a] | 28.1 | 864 | 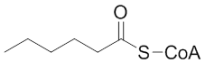 |
| heptanoic acid[a] | 32.9 | 878 | 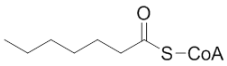 |
| octanoic acid[a] | 38.8 | 892 | 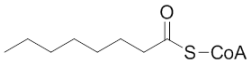 |
| nonanoic acid[a] | 43.2 | 906 | 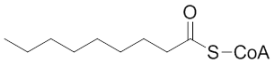 |
| (*E*)-2-hexenoic acid[b] | 10.8 | 862 | 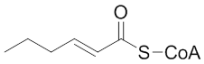 |
| (*E*)-2-heptenoic acid[b] | 13.4 | 876 | 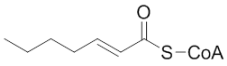 |
| (*E*)-2-octenoic acid[b] | 16.4 | 890 | 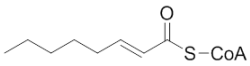 |
| (*E*)-2-nonenoic acid[b] | 19.9 | 904 | 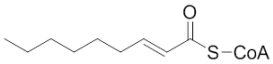 |
| (*E*)-2-decenoic acid[b] | 24.2 | 918 | 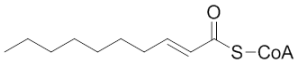 |
| (*E*)-2-undecenoic acid[b] | 28.9 | 932 | 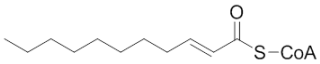 |
| (*E*)-3-pentenoic acid[c] | 18.5 | 848 | 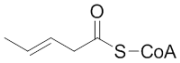 |
| (*E*)-3-hexenoic acid[c] | 23.4 | 862 | 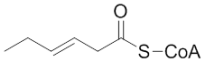 |
| (*E*)-3-heptenoic acid[c] | 29.3 | 876 | 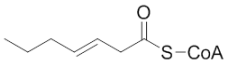 |
| (*E*)-3-octenoic acid[c] | 34.2 | 890 | 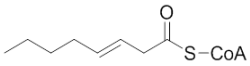 |
| (*E*)-3-nonenoic acid[c] | 39.2 | 904 | 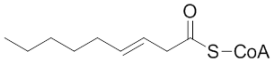 |
| (*E*)-3-decenoic acid[c] | 45.2 | 918 | 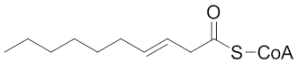 |

[a] Eluted by a linear gradient from 2–20% acetonitrile for saturated acyl-CoA.
[b] Eluted by a linear gradient from 2–50% acetonitrile for (*E*)-2-enoyl-CoA.
[c] Eluted by a linear gradient from 2–65% acetonitrile for (*E*)-3-enoyl-CoA.

**TABLE 3**
**Kinetic constants of RevS for fatty acids, ATP, and CoA.**

| Enzyme | Substrate | $K_m$ | $k_{cat}$ | $k_{cat}/K_m$ |
|---|---|---|---|---|
| | | mM | $min^{-1}$ | $mM^{-1}$ $min^{-1}$ |
| RevS | hexanoic acid | 0.32 ± 0.07 | 5.2 ± 0.3 | 16 |
| | heptanoic acid | 0.26 ± 0.03 | 18.3 ± 0.5 | 70 |
| | octanoic acid | 0.32 ± 0.04 | 43.5 ± 1.5 | 136 |
| | nonanoic acid | 0.48 ± 2.44 | 44.3 ± 0.1 | 92 |
| | decanoic acid | 0.31 ± 0.02 | 19.6 ± 0.3 | 64 |
| | (*E*)-2-hexenoic acid | 0.59 ± 0.05 | 5.5 ± 0.2 | 9.3 |
| | (*E*)-2-heptenoic acid | 0.57 ± 0.05 | 15.1 ± 0.4 | 27 |
| | (*E*)-2-octenoic acid | 0.49 ± 0.07 | 35.8 ± 1.5 | 74 |
| | (*E*)-2-nonenoic acid | 0.48 ± 0.04 | 49.5 ± 1.2 | 103 |
| | (*E*)-2-decenoic acid | 0.30 ± 0.04 | 19.3 ± 0.7 | 65 |
| | (*E*)-2-undecenoic acid | 0.075 ± 0.004 | 6.6 ± 0.1 | 88 |
| | (*E*)-3-hexenoic acid | 0.95 ± 0.11 | 14.2 ± 0.6 | 15 |
| | (*E*)-3-heptenoic acid | 0.47 ± 0.06 | 18.2 ± 0.7 | 39 |
| | (*E*)-3-octenoic acid | 0.51 ± 0.92 | 41.3 ± 0.9 | 81 |
| | (*E*)-3-nonenoic acid | 0.71 ± 1.19 | 59.6 ± 1.1 | 85 |
| | (*E*)-3-decenoic acid | 0.38 ± 0.03 | 23.6 ± 0.6 | 62 |
| | CoA[a] | 0.05 ± 0.01 | 39.6 ± 0.8 | 861 |
| | ATP[a] | 0.039 ± 0.004 | 56.7 ± 2.2 | 1456 |
| Mig[b] | octanoic acid | 0.285 | 11 | 38 |
| | CoA[a] | 0.045 | | |
| | ATP[a] | 0.036 | | |
| FadD13[c] | palmitic acid | 0.019 ± 0.005 | 1.66 | 87.3 |
| | CoA[d] | 0.13 ± 0.01 | | |
| | ATP[d] | 0.24 ± 0.05 | | |

At least triplicate assays were performed. The data represents mean ± S.E.M. The $k_{cat}/K_m$ value was calculated based on the mean value of value $K_m$ and $k_{cat}$.
[a] Octanoic acid was used as a substrate.
[b] Kinetic parameter reported by Morsczeck *et al*. (65).
[c] Kinetic parameter reported by Khare *et al*. (66).
[d] Palmitic acid was used as a substrate (66).

**TABLE 4**
**Comparison of the kinetic constant of RevT and CCR homologs reported**

| Enzyme | Substrate | $K_m$ | $k_{cat}$ | $k_{cat}/K_m$ |
|---|---|---|---|---|
| | | mM | $min^{-1}$ | $mM^{-1}$ $min^{-1}$ |
| RevT | (*E*)-2-hexenoyl-CoA | 0.27 ± 0.01 | 28.3 ± 0.5 | 104 |
| | (*E*)-2-octenoyl-CoA | 0.33 ± 0.04 | 36.2 ± 1.3 | 109 |
| | NADPH[a] | 0.12 ± 0.01 | 33.9 ± 1.5 | 282 |
| | NADPH[b] | 0.12 ± 0.01 | 41.1 ± 2.0 | 342 |
| SalG[c] | crotonyl-CoA | 0.0207 ± 0.0042 | 15.4 ± 0.9 | 744 |
| | chlorocrotonyl-CoA | 0.0044 ± 0.0018 | 23.1 ± 2.6 | 5250 |
| CinF[d] | crotonyl-CoA | 0.95 ± 0.05 | 82.6 ± 4.4 | 86.6 |
| | (*E*)-2-octenoyl-CoA | 0.23 ± 0.01 | 17.4 ± 1.1 | 75.7 |
| SpnE[e] | crotonyl-CoA | 0.36 ± 0.03 | 0.218 ± 0.011 | 0.614 |
| | cinnamoyl-CoA | 0.078 ± 0.002 | 0.112 ± 0.006 | 1.43 |

At least triplicate assays were performed. The data represents mean ± S.E.M. The $k_{cat}/K_m$ value was calculated based on the mean value of value $K_m$ and $k_{cat}$.
[a] (*E*)-2-hexenoyl-CoA was used as a substrate.
[b] (*E*)-2-octenoyl-CoA was used as a substrate.
[c] Kinetic parameter reported by Eustáquio *et al*. (27).
[d] Kinetic parameter reported by Quade *et al*. (31).
[e] Kinetic parameter reported by Chang *et al*. (67).

Fig. 1

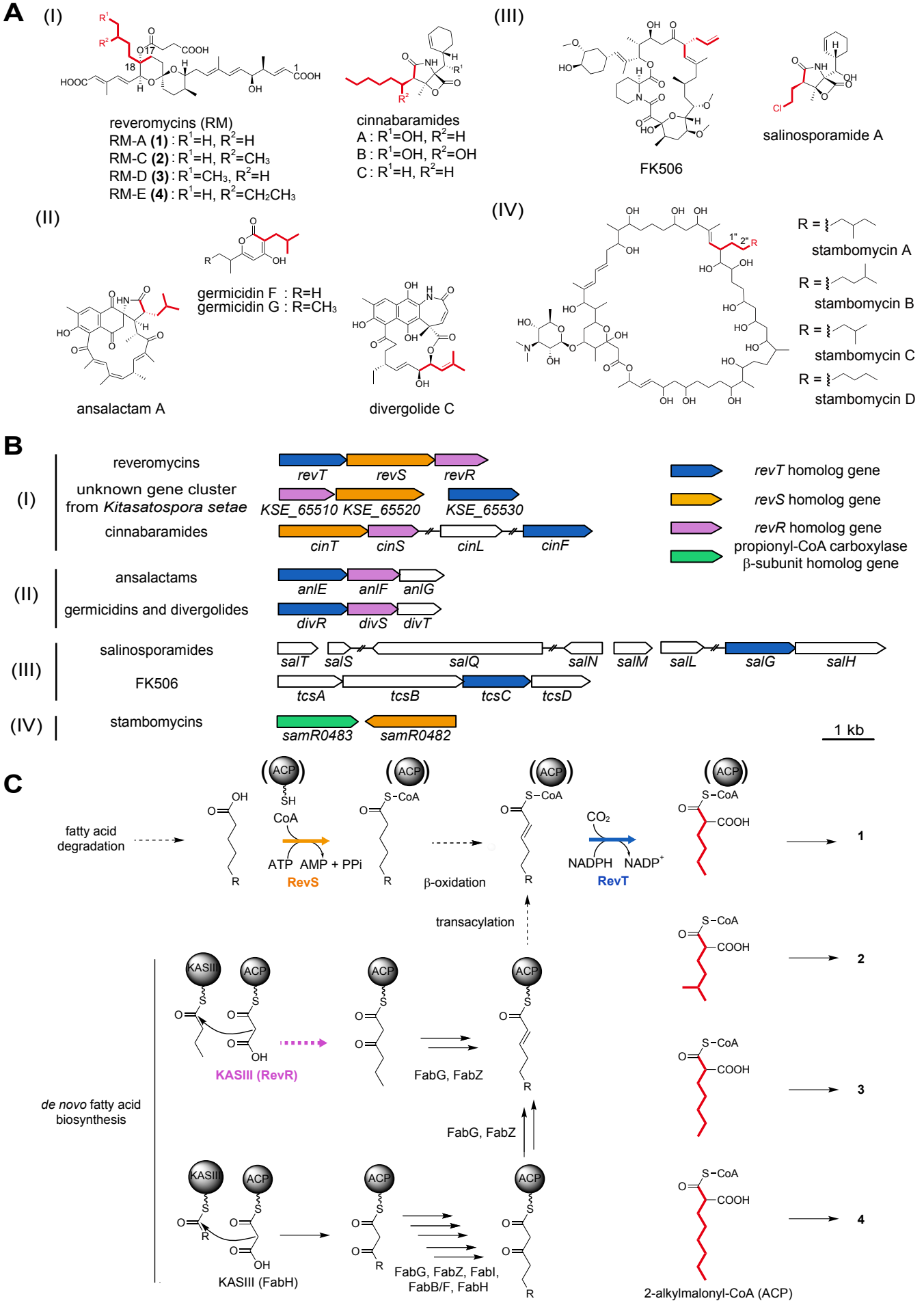
A
(I)
reveromycins (RM)
RM-A (1) : R1=H, R2=H
RM-C (2) : R1=H, R2=CH3
RM-D (3) : R1=CH3, R2=H
RM-E (4) : R1=H, R2=CH2CH3
cinnabaramides
A : R1=OH, R2=H
B : R1=OH, R2=OH
C : R1=H, R2=H
(II)
germicidin F : R=H
germicidin G : R=CH3
ansalactam A
divergolide C
(III)
FK506
salinosporamide A
(IV)
stambomycin A
stambomycin B
stambomycin C
stambomycin D
B
(I)
reveromycins
revT revS revR
unknown gene cluster from Kitasatospora setae
KSE_65510 KSE_65520 KSE_65530
cinnabaramides
cinT cinS cinL cinF
revT homolog gene
revS homolog gene
revR homolog gene
propionyl-CoA carboxylase β-subunit homolog gene
(II)
ansalactams
anlE anlF anlG
germicidins and divergolides
divR divS divT
(III)
salinosporamides
salT salS salQ salN salM salL salG salH
FK506
tcsA tcsB tcsC tcsD
(IV)
stambomycins
samR0483 samR0482
1 kb
C
fatty acid degradation
ACP
CoA
ATP AMP + PPi
RevS
β-oxidation
CO2
NADPH NADP+
RevT
transacylation
KASIII
KASIII (RevR)
FabG, FabZ
de novo fatty acid biosynthesis
KASIII (FabH)
FabG, FabZ, FabI, FabB/F, FabH
2-alkylmalonyl-CoA (ACP)
1
2
3
4

# Fig. 2

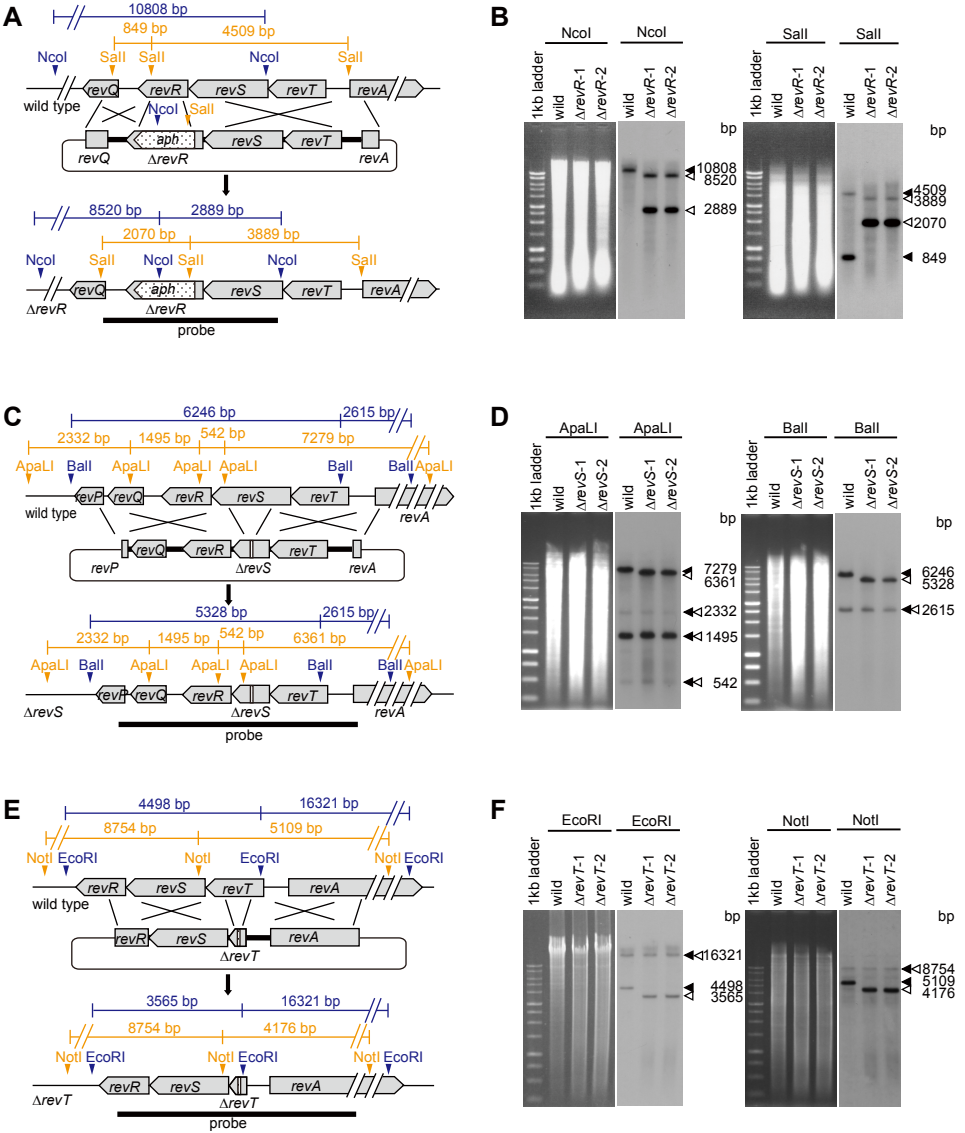
A
10808 bp
849 bp
4509 bp
NcoI
SalI
SalI
NcoI
SalI
revQ
revR
revS
revT
revA
wild type
NcoI
SalI
aph
revS
revT
revQ
ΔrevR
revA
8520 bp
2889 bp
2070 bp
3889 bp
NcoI
SalI
NcoI
SalI
NcoI
SalI
revQ
aph
revS
revT
revA
ΔrevR
ΔrevR
probe
B
NcoI
NcoI
SalI
SalI
1kb ladder
wild
ΔrevR-1
ΔrevR-2
bp
10808
8520
2889
4509
3889
2070
849
C
6246 bp
2615 bp
2332 bp
1495 bp
542 bp
7279 bp
ApaLI
BalI
ApaLI
ApaLI
ApaLI
BalI
BalI
ApaLI
revP
revQ
revR
revS
revT
revA
wild type
revQ
revR
revT
revP
ΔrevS
revA
5328 bp
2615 bp
2332 bp
1495 bp
542 bp
6361 bp
ApaLI
BalI
ApaLI
ApaLI
ApaLI
BalI
BalI
ApaLI
revP
revQ
revR
revT
ΔrevS
ΔrevS
revA
probe
D
ApaLI
ApaLI
BalI
BalI
1kb ladder
wild
ΔrevS-1
ΔrevS-2
bp
7279
6361
2332
1495
542
6246
5328
2615
E
4498 bp
16321 bp
8754 bp
5109 bp
NotI
EcoRI
NotI
EcoRI
NotI
EcoRI
revR
revS
revT
revA
wild type
revR
revS
revA
ΔrevT
3565 bp
16321 bp
8754 bp
4176 bp
NotI
EcoRI
NotI
EcoRI
NotI
EcoRI
ΔrevT
revR
revS
revA
ΔrevT
probe
F
EcoRI
EcoRI
NotI
NotI
1kb ladder
wild
ΔrevT-1
ΔrevT-2
bp
16321
4498
3565
8754
5109
4176

Fig. 3

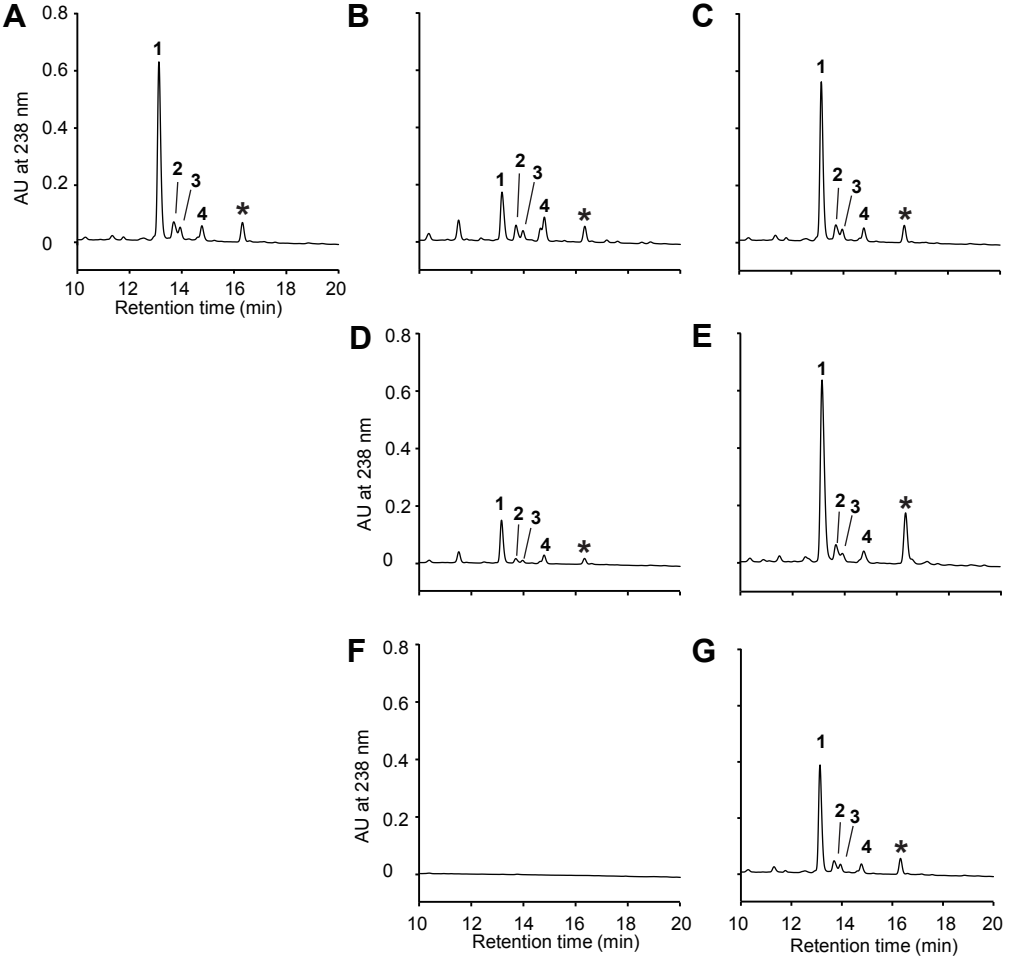
A
B
C
D
E
F
G
AU at 238 nm
Retention time (min)
0
0.2
0.4
0.6
0.8
10
12
14
16
18
20
1
2
3
4
*

# Fig. 4

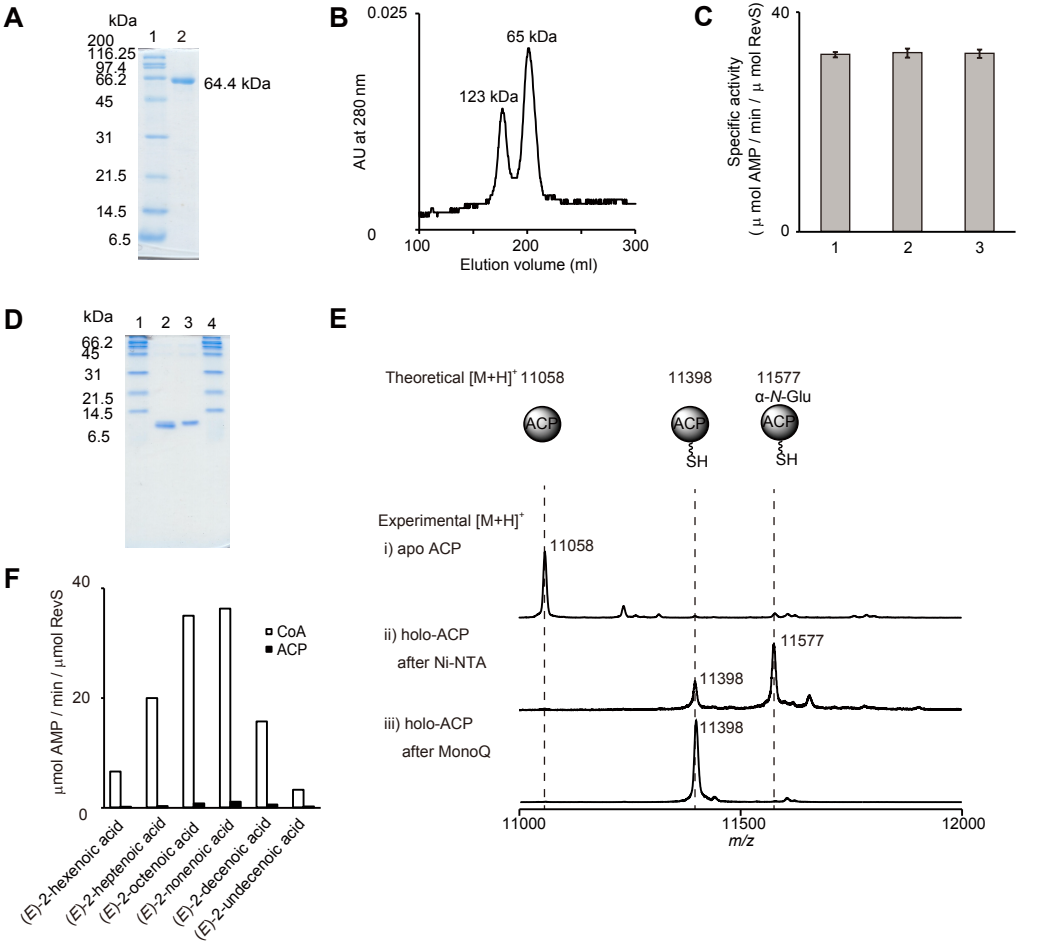
A
kDa
1
2
200
116.25
97.4
66.2
45
31
21.5
14.5
6.5
64.4 kDa
B
0.025
0
AU at 280 nm
65 kDa
123 kDa
100
200
300
Elution volume (ml)
C
40
0
Specific activity
( μ mol AMP / min / μ mol RevS)
1
2
3
D
kDa
1
2
3
4
66.2
45
31
21.5
14.5
6.5
E
Theoretical [M+H]+ 11058
11398
11577
α-N-Glu
ACP
ACP
ACP
SH
SH
Experimental [M+H]+
i) apo ACP
11058
ii) holo-ACP
after Ni-NTA
11577
11398
iii) holo-ACP
after MonoQ
11398
11000
11500
12000
m/z
F
40
20
0
μmol AMP / min / μmol RevS
CoA
ACP
(E)-2-hexenoic acid
(E)-2-heptenoic acid
(E)-2-octenoic acid
(E)-2-nonenoic acid
(E)-2-decenoic acid
(E)-2-undecenoic acid

Fig. 5

A

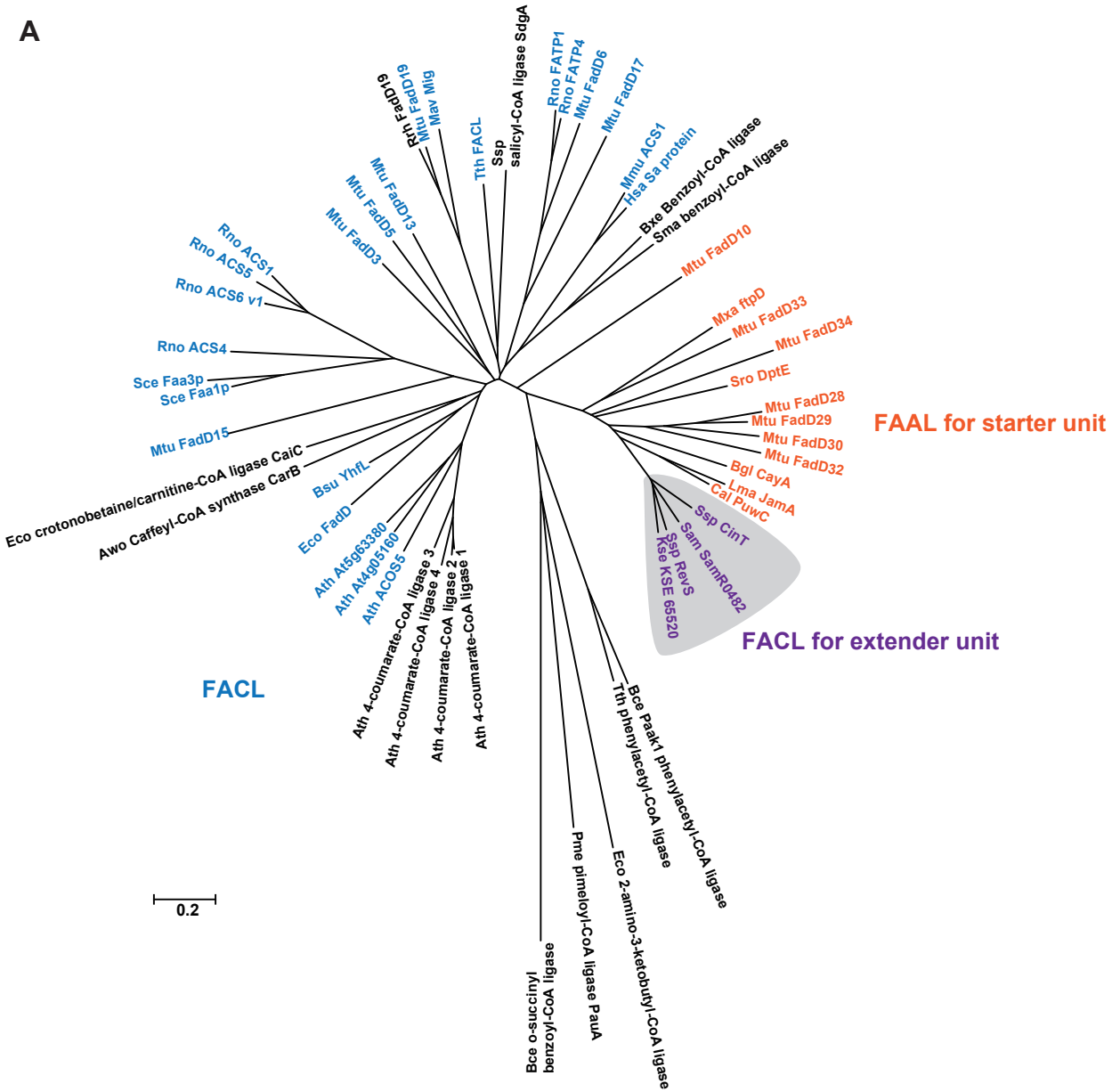


B

fatty acyl AMP ligase specific insertion

```
Ssp RevS     CPGYGLAENTLKLSGSPEDRPPTLLRADAAALQDGRVVPLTGPGTDGVRLVGSGV 377
Mtu FadD28   RPSYGLAEATVYVATSKPGQPPETVDFDTESLSAGHAKPCAGG---GATSLISYM 377
Lpn FAAL     YPCYGLAEATLLVTGGTPGSSYKTLTLAKEQFQDHRVHFADDNSPGSYKLVSSGN 376
Eco FAAL     MPCYGLAENALAVSFSDEASGVVVNEVDRDILEYQGKAVAPGAETRAVSTFVNCG 388
Tth FACL     RQGYGLTETSPVVVQNFVKSHLE---------------SLSEEEKLTLKAKTGLP 360
Set FACL     VDTWWQTETGGFMITPLPGAIE--------------------------LKAGSAT 438
Mtu FadD19   TDSIGSSETGFGGTSVVAAGQAH---------------------------GGGPR 354
```

# Fig. 6

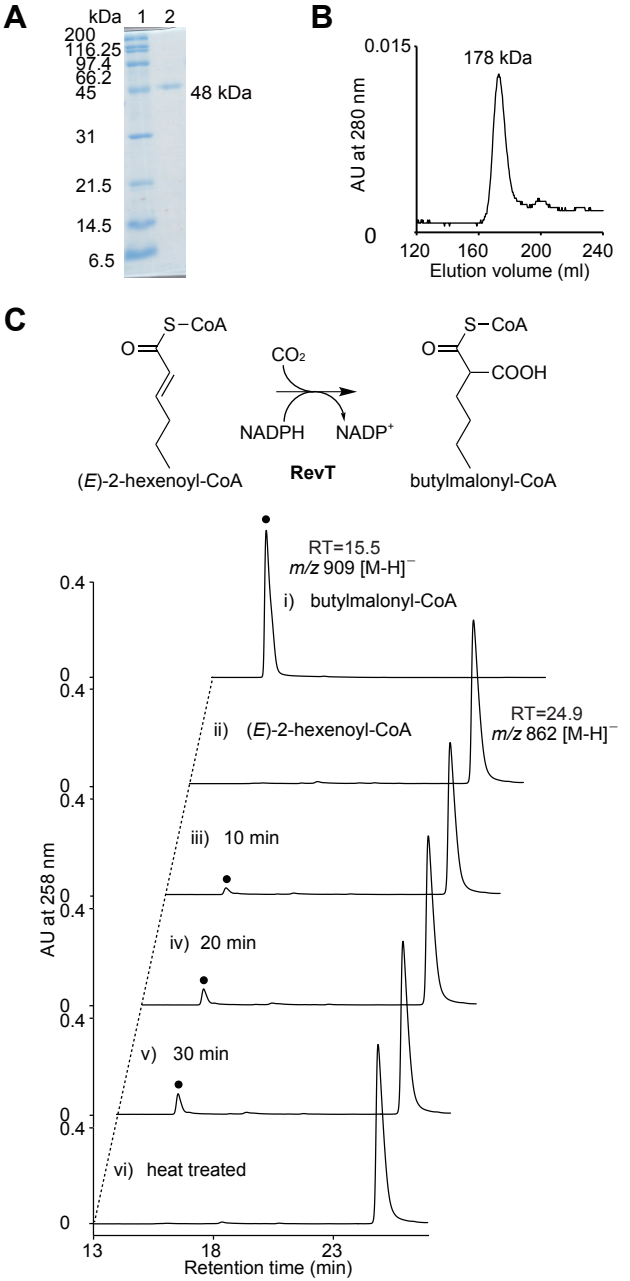
A
kDa 1 2
200
116.25
97.4
66.2
45
31
21.5
14.5
6.5
48 kDa
B
0.015
178 kDa
AU at 280 nm
0
120 160 200 240
Elution volume (ml)
C
S−CoA
O
(E)-2-hexenoyl-CoA
CO2
NADPH
NADP+
RevT
S−CoA
O
COOH
butylmalonyl-CoA
RT=15.5
m/z 909 [M-H]−
i) butylmalonyl-CoA
RT=24.9
m/z 862 [M-H]−
ii) (E)-2-hexenoyl-CoA
iii) 10 min
iv) 20 min
v) 30 min
vi) heat treated
AU at 258 nm
0.4
0
13 18 23
Retention time (min)

Fig. 7

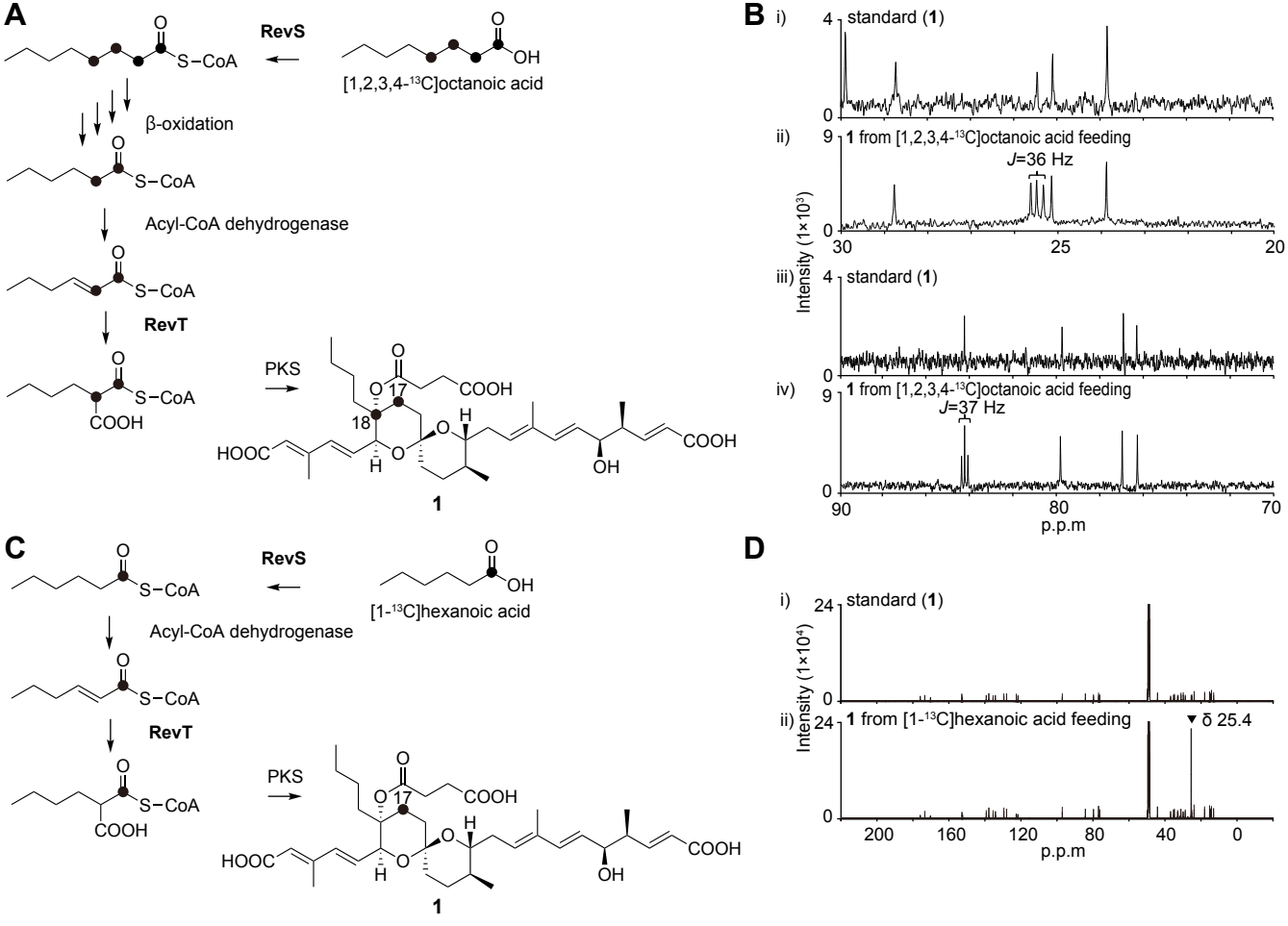
A
RevS
[1,2,3,4-13C]octanoic acid
β-oxidation
Acyl-CoA dehydrogenase
RevT
PKS
1
B
i) standard (1)
ii) 1 from [1,2,3,4-13C]octanoic acid feeding
J=36 Hz
iii) standard (1)
iv) 1 from [1,2,3,4-13C]octanoic acid feeding
J=37 Hz
Intensity (1×10³)
p.p.m
C
RevS
[1-13C]hexanoic acid
Acyl-CoA dehydrogenase
RevT
PKS
1
D
i) standard (1)
ii) 1 from [1-13C]hexanoic acid feeding
δ 25.4
Intensity (1×10⁴)
p.p.m

Fig. 8

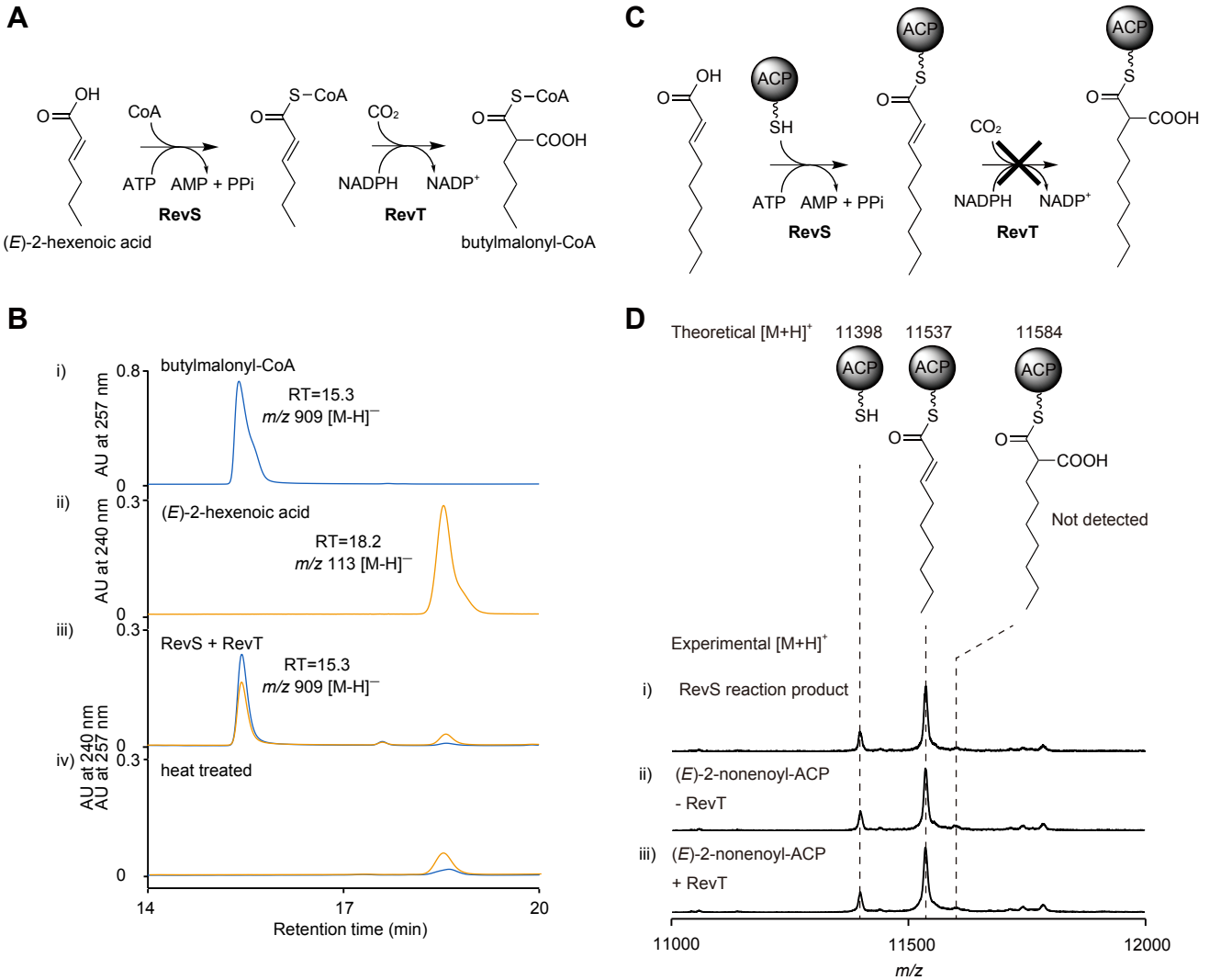
A
OH
O
CoA
ATP
AMP + PPi
RevS
S−CoA
O
CO₂
NADPH
NADP⁺
RevT
S−CoA
O
COOH
(E)-2-hexenoic acid
butylmalonyl-CoA
B
i)
butylmalonyl-CoA
RT=15.3
m/z 909 [M-H]⁻
AU at 257 nm
0.8
0
ii)
(E)-2-hexenoic acid
RT=18.2
m/z 113 [M-H]⁻
AU at 240 nm
0.3
0
iii)
RevS + RevT
RT=15.3
m/z 909 [M-H]⁻
0.3
0
iv)
heat treated
AU at 240 nm
AU at 257 nm
0.3
0
14
17
20
Retention time (min)
C
OH
O
ACP
SH
ATP
AMP + PPi
RevS
ACP
S
O
CO₂
NADPH
NADP⁺
RevT
ACP
S
O
COOH
D
Theoretical [M+H]⁺
11398
11537
11584
ACP
SH
ACP
S
O
ACP
S
O
COOH
Not detected
Experimental [M+H]⁺
i)
RevS reaction product
ii)
(E)-2-nonenoyl-ACP
- RevT
iii)
(E)-2-nonenoyl-ACP
+ RevT
11000
11500
12000
m/z

Enzymology:

# Identification of middle chain fatty acyl-CoA ligase responsible for the biosynthesis of 2-alkylmalonyl-CoAs for polyketide extender unit



Takeshi Miyazawa, Shunji Takahashi, Akihiro Kawata, Suresh Panthee, Teruo Hayashi, Takeshi Shimizu, Toshihiko Nogawa and Hiroyuki Osada

*J. Biol. Chem. published online September 16, 2015*